TRANSFEMORAL PROSTHESIS CONTROL FOR INCLINED WALKING USING IMPEDANCE CONTROL AND BEZIER POLYNOMIAL BASED OPTIMIZATION

A Thesis

by

WOOLIM HONG

Submitted to the Office of Graduate and Professional Studies of
Texas A&M University
in partial fulfillment of the requirements for the degree of

MASTER OF SCIENCE

Chair of Committee,	Shankar P. Bhattacharyya
Co-Chair of Committee,	Pilwon Hur
Committee Members,	Aniruddha Datta
	Hamid A. Toliyat
Head of Department,	Miroslav M. Begovic

December 2017

Major Subject: Electrical Engineering

ABSTRACT

A powered transfemoral prosthesis is an assistive device for patients with above knee amputation. For these patients, walking on various sloped surfaces is one of the most challenging tasks in their daily lives. Designing prostheses that can effectively adapt to varying terrain remains an ordeal to this date. In this thesis, we focused on generating the desired trajectories for various inclined surfaces without prior knowledge of slopes using human impedance and cubic-Bezier-polynomials-based optimization. Trajectory generation for the powered prosthesis is an important procedure to design an appropriate controller that mimics human locomotion; the trajectory has to be generated for each gait cycle in real-time to produce a stable, robust, and human-like walking. The proposed method is rooted in analyzing the human data from the motion capture system, to gain an understanding of how human walks differently according to the slopes. Impedance control using human parameters allows the prosthesis adapt to these different slopes during the stance phase. Since impedance control is used only during the stance phase, we were prompted to consider a different control strategy for the swing phase. These trajectories are tracked using PD control. Thus, we proposed the cubic-Bezier-curve-based optimization to generate appropriate trajectories for the given slopes during the swing phase, without any information regarding the slopes. Before the heel contact occurs (terminal swing phase), low gain PD control is used to adapt to the unexpected slopes and smoothly track the generated trajectories. To validate the proposed framework, the concept was implemented on a transfemoral prosthesis, *AMPRO II*, on various slopes. The main objective of the thesis is to propose and verify a unified framework that enables the transfemoral prosthesis to perform real-time inclined walking without a priori information regarding the terrain.

DEDICATION

This work is dedicated to my family. They have sincerely supported me with all their hearts and greate care. I couldn't have done this work without their support and prayers.

And above all,

To the Almighty God, who always lights my way.

ACKNOWLEDGMENTS

I would like to thank my advisor in the electrical & computer engineering department, Dr. Shankar P. Bhattacharyya, for all his support to finish my research. I would also like to thank my other advisor in the mechanical engineering department, Dr. Pilwon Hur, for letting me join HUR (Human Rehabilitation) Group and his careful guidance that he has given me over the past two years. I would like to express my gratitude to my committee members, Dr. Aniruddha Datta and Dr. Hamid A. Toliyat, for their valuable comments on my research. Finally, I would also like to acknowledge all members of the HUR Group specially including Victor Christian Paredes Cauna, for their sincere support and great help to finish my research successfully. The warmth that all of my friends has shown has encouraged me and allowed me to take another step when I was exhausted.

CONTRIBUTORS AND FUNDING SOURCES

Contributors

This work was supported by a thesis committee consisting of Professor Dr. Shankar P. Bhattacharyya of the Department of Electrical & Computer Engineering and Dr. Pilwon Hur of the Department of Mechanical Engineering, and Dr. Aniruddha Datta, Dr. Hamid A. Toliyat of the Department of Electrical & Computer Engineering.

All other work conducted for the thesis was completed by the student independently.

Funding Sources

Graduate study was supported by a scholarship from the Electrical & Computer Engineering Department, and also supported by the Mechanical Engineering Department at Texas A&M University.

NOMENCLATURE

OGAPS	Office of Graduate and Professional Studies at Texas A&M University
B/CS	Bryan/College Station
HSUS	Human Society of the United States
TAMU	Texas A&M University
ACA	Amputee Coalition of America
COM	Center of Mass
HIC	Human Inspired Control
CWF	Canonical Walking Function
HZD	Hybrid Zero Dynamics
PHZD	Partial Hybrid Zero Dynamics
AMPRO I	A&M Prosthesis, ver.1
AMPRO II	A&M Prosthesis, ver.2
PD	Proportional and Derivative
PCA	Principal Component Analysis
IMU	Inertial Measurement Unit
CAN	Controller Area Network
PPI	Piecewise Passive Impedance
HIA	Hybrid Impedance-Admittance

TABLE OF CONTENTS

Page

ABSTRACT ii

DEDICATION iii

ACKNOWLEDGMENTS iv

CONTRIBUTORS AND FUNDING SOURCES v

NOMENCLATURE vi

TABLE OF CONTENTS vii

LIST OF FIGURES ix

1. INTRODUCTION 1

    1.1 AMPRO II 8
    1.2 Thesis Structure 9

2. RESEARCH OBJECTIVES 11

3. HUMAN MOTION ANALYSIS FOR INCLINED WALKING 12

    3.1 Human Data Analysis for Inclined Walking 12
        3.1.1 Human walking data 12
        3.1.2 Flat-ground walking 14
        3.1.3 Upslope walking 15
        3.1.4 Downslope walking 16

4. PROSTHESIS CONTROL STRATEGY FOR INCLINED WALKING 18

    4.1 Prosthesis Strategy for Inclined Walking 18
        4.1.1 Stability of walking with prosthesis 19
            4.1.1.1 Stability of the periodic orbit 19
            4.1.1.2 Human-inspired control 23
            4.1.1.3 Stability of human walking 27
        4.1.2 Synchronization of step progression 27
    4.2 Impedance-Based Control 31

4.3 Cubic-Bezier-Polynomials-Based Optimization 33

5. RESULTS 40

5.1 Bezier-Polynomials-Based Optimization Results 40
5.2 Experimental Set-up & Protocol 42
5.2.1 Indoor experiment protocol 42
5.3 Experimental Results 42

6. FUTURE WORKS 51

7. CONCLUSION & DISCUSSION 52

REFERENCES 53

LIST OF FIGURES

FIGURE Page

1.1 5 different levels of lower limb amputation [1] 1

1.2 Ottobock 3WR95, the aqualine waterproof passive prosthesis [2]..... 3

1.3 Ottobock C-Leg, the micro-processor prosthetic system designed to reproduce the functions of a biological leg [3] 4

1.4 Center of Intelligent Mechatronics at Vanderbilt University, the powered prosthetic system designed to provide the net power for the ankle and knee joints [4] 4

1.5 AMPRO I, the powered transfemoral prosthesis developed in Texas A&M University [5]..... 6

1.6 AMPRO II is the second version powered transfemoral prosthesis developed at Texas A&M University. 8

3.1 The knee joint rotates in two direction: flexion and extension, while the ankle joint moves in two directions: dorsiflexion and plantar flexion 12

3.2 Bio-mechanical analysis for human walking can be done by utilizing camera-based motion capture system. (14 reflective markers were used)..... 13

3.3 Joint angle trajectories for flat-ground walking (A: ankle joint angle, B: knee joint angle)..... 14

3.4 Joint angle trajectories for upslope walking compared to the flat-ground walking trajectory (0°, 5°, 10°, and 15°)
(A: ankle joint angle, B: knee joint angle) 16

3.5 Joint angle trajectories for downslope walking compared to the flat-ground walking trajectory (-15°, -10°, -5°, and 0°)
(A: ankle joint angle, B: knee joint angle) 17

4.1 Two different strategies to the robotic system for inclined walking 18

4.2 The basic concept of Poincare map 19

4.3 3-Dimensional phase portrait during 4 steps of human on flat-ground 20

4.4 2-Dimensional phase portrait during 4 steps of human on flat-ground 21

4.5 Poincare map is constructed in the phase portrait of human walking gait cycle..... 22

4.6 7-link bipedal robotic model which is inspired from human [6]..... 23

4.7 The change of IMU sensor position can provide more practical usage of the prosthesis to the users. 28

4.8 The movement of a global thigh angle during a gait cycle on the sloped surfaces 29

4.9 The relationship between the normalized thigh angle and its integral can be represented as a circular trend in quadrants..... 30

4.10 The phase variable from thigh angle is bounded in [0,1]..... 30

4.11 Varying impedance parameters, which is dependent on the time parameter from the phase variable 33

4.12 Using Bezier polynomials to generate the appropriate inclined walking trajectories 34

4.13 Bezier curve based optimization with human data (H)..... 34

4.14 Re-describing P_1, P_2 by considering the smoothness constraints 36

5.1 Comparison between human ankle data and the results of Bezier based optimization problem
A: Ankle angle trajectories on 0° – 15° slopes in 60%–85% of a gait cycle
B: Plot A with the generated trajectories from the optimization results
C: Ankle angle trajectories on -15° – 0° slopes in 60%–85% of a gait cycle
D: Plot C with the generated trajectories from the optimization results..... 40

5.2 Comparison between human knee data and the results of Bezier based optimization problem
A: Knee angle trajectories on 0° – 15° slopes in 60%–85% of a gait cycle
B: Plot A with the generated trajectories from the optimization results
C: Knee angle trajectories on -15° – 0° slopes in 60%–85% of a gait cycle
D: Plot C with the generated trajectories from the optimization results..... 41

5.3 Comparison between the prosthesis' and the human walking on -10° inclination (A: Ankle joint, B: Knee joint) 43

5.4 Comparison between the prosthesis' and the human walking on -5° inclination (A: Ankle joint, B: Knee joint) 44

5.5 Comparison between the prosthesis' and the human walking on Flat-ground (A: Ankle joint, B: Knee joint) 44

5.6 Comparison between the prosthesis' and the human walking on 5° inclination (A: Ankle joint, B: Knee joint) 45

5.7 Comparison between the prosthesis' and the human walking on 10° inclination (A: Ankle joint, B: Knee joint) 45

5.8 Downslope walking on the treadmill (-10° inclination) 46

5.9 Downslope walking on the treadmill (-5° inclination) 47

5.10 Flat-ground walking on the treadmill 48

5.11 Upslope walking on the treadmill (5° inclination)..... 49

5.12 Upslope walking on the treadmill (10° inclination) 50

1. INTRODUCTION

Amputation is typically known to affect the victims adversely - be it psychologically and physically. In particular, lower extremity amputation results in the reduction of amputees' mobility and dexterity in their daily lives – making patients vulnerable to fall and resulting injuries [7]. Even though these people are not able to walk as they did before the amputation, they still have a chance to recover their locomotion by using an assistive device, such as a prosthetic leg. This motivates us to develop a lower limb prosthesis that performs human-like walking.

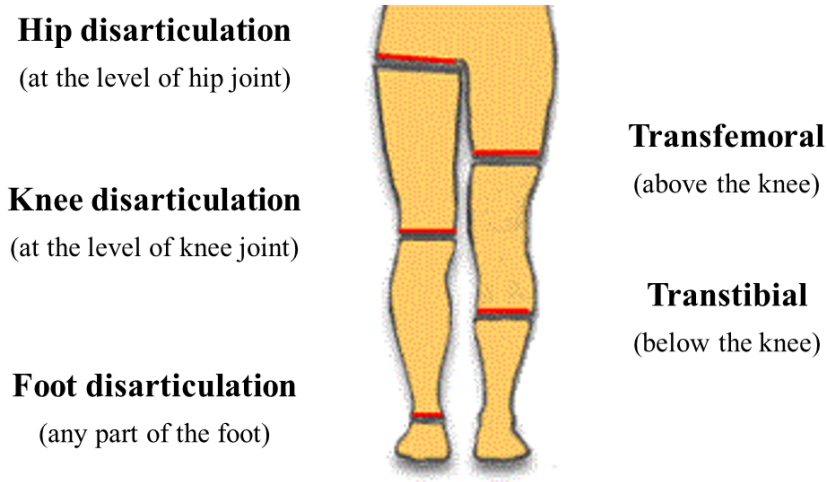

Figure 1.1: 5 different levels of lower limb amputation [1]

Lower limb amputation can be categorized into five types (Fig.1.1): foot amputation (amputation of any part of the foot), transtibial (amputation below the knee), knee disarticulation (amputation at the level of the knee joint), transfemoral (amputation above the

knee), and hip disarticulation (amputation at the level of the hip joint) [1]. According to the National Center for Health Statistics, transfemoral amputees account for 18.5% of 1.2 million amputees in the United States [8]. As per a report by the Healthcare Cost and Utilization Project from 1988 through 1996, transfemoral amputees are the 2nd largest group (transtibial amputees are the largest group) among the lower limb amputations except toe amputation [9]; toe amputation is normally excluded from consideration while developing prostheses because toe prostheses are barely needed for the amputees. It is also shown in a case study conducted by Johns Hopkins University, in collaboration with the Amputee Coalition of America (ACA), transtibial amputees form the largest group of lower limb amputation, followed by transfemoral amputees [10]. Between these two most common amputees, transfemoral amputees face more mobility challenges and are more prone to falls than transtibial amputees.

Due to the investigation of transtibial prostheses in the research field, high-performing transitibial prostheses have been developed. A transitibial prosthesis is developed in Michigan Tech, has two controllable degrees of freedom including dorsiflexion & plantar flexion, and inversion & eversion by using a cable-driven mechanism to provide more human-like ankle characteristics during a step [11]. With more degrees of freedom, amputees have more authority over the prosthesis' reaction to unexpected situations during operation. Beyond the daily activities, some cutting edge transtibial prosthesis can provide more freedom for amputees to express their artistic emotion such as dance [12]. Furthermore, to contribute to more human-like walking gait, there is on-going research which focuses on designing a toe joint enable push-off toe [13]. Honert *et al.*, addressed adding an elastic toe joint to enhance the push-off capability by comparing two different versions (with an elastic toe joint vs. without a toe joint) of customized prosthetic foot and by studying how adding a toe joint affects Center of Mass (COM) and push-off power [13].

Figure 1.2: Ottobock 3WR95, the aqualine waterproof passive prosthesis [2]

Despite these efforts in transtibial prostheses, transfemoral prostheses still have lots of challenges than transtibial prostheses. The most distinct and difficult part of developing transfemoral prostheses is ensuring stability. Since the transfemoral prostheses should perform more functions (including those of the knee joint) than transtibial prostheses, they are more prone to cause falls when the systems malfunction. Therefore, the stability problem should be more carefully handled. The transfemoral prostheses can be classified under three categories: i) passive prostheses, ii) micro-processor prostheses, and iii) powered prostheses. Passive prostheses (Fig.1.2), the classic, are the most commonly used type because they are light weight and easy to operate. But, they do not compensate for the power loss associated with a missing limb. Micro-processor prostheses, such as C-Leg (Fig.1.3) enable amputees to alter the damping properties of the prosthetic as per the task at hand – thus, making them a popular choice [3]. While micro-processor prostheses pro-

Figure 1.3: Ottobock C-Leg, the micro-processor prosthetic system designed to reproduce the functions of a biological leg [3]

Figure 1.4: Center of Intelligent Mechatronics at Vanderbilt University, the powered prosthetic system designed to provide the net power for the ankle and knee joints [4]

vide power only to the knee, powered prostheses (Fig.1.4) can contribute to the amputees' walking by providing net power during the gait cycle to both the knee and the ankle. Since powered prosthesis uses sensor data from the user, real-time feedback control can be used to generate human-like walking gait.

Since we are dealing with a robotic system attached to the human body, it is imperative for the system not to interrupt human walking. Therefore, transfemoral prostheses are expected to perform a stable human-like locomotion under normal circumstances, such as flat ground and inclined terrains. However, existing passive and micro-processor prostheses cannot fully accommodate such functions because they cannot control the system adaptively. To satisfy user expectation, there have been several studies on transfemoral amputees to develop an effective powered transfemoral prostheses. Fig.1.4 shows the prosthesis developed by Vanderbilt University. It is based on impedance control and trajectory tracking, using the set of impedance parameters along the user's walking [4]. In order to successfully control the prosthesis, they decomposed the gait cycle into several states, and specify the different linear stiffness and damping coefficients to each state. Each state generates torques for each joint that ensure passivity within these states [14]. They also expanded this approach to upslope walking [15] and stair walking [16] by adding different modes to the system. By using motion capture data, they analysed human walking trend on stairs and found the conditions for state transitions for stair walking, which were further used to implement to a finite state-based control system [16]. For every single situation, Vanderbilt prosthesis is required to tune the impedance parameters based on the joint sensor. The set of parameters that they used vary based on the user, thus mandating a tuning process prior operation. This can limit the practical usage of the prosthesis.

AMBER Lab (now at California Institute of Technology) proposed Human-Inspired Control (HIC) to avoid the tuning process by using optimized Canonical Walking Functions (CWF) (Fig.1.5). HIC is a framework based on Hybrid Zero Dynamics (HZD),

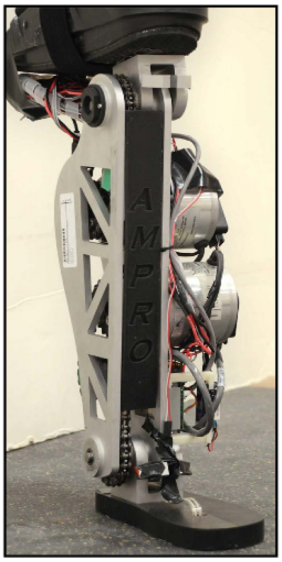

Figure 1.5: AMPRO I, the powered transfemoral prosthesis developed in Texas A&M University [5]

which is the mathematical description of hybrid systems including a discrete heel contact event and continuous human walking [17]. Yet, it is necessary to relax some constraints to avoid high velocity jump at the knee when the heel strike happens. Therefore, Partial Hybrid Zero Dynamics (PHZD) is proposed to automatically generate stable and human-like walking trajectories [18]. This framework has the advantage of being mathematically stable owing to PHZD [18], [19]; because of this advantage, it is widely used in bipedal robotics and prostheses [19], [20]. However, to generate the trajectories which satisfy PHZD conditions, a heavy optimization problem, which is a computationally demanding process must be solved. To overcome this difficulty, a previous study using convex optimization based spline generation was proposed to generate upslope and flat ground walking trajectories in real-time [6]. The advantage of this method is the ability to perform flat ground and upslope walking without any slope information by adapting to the slope with low gain PD control and blending into the flat ground walking trajectory with spline generation. This algorithm allows us to avoid solving heavy optimization problem and tuning

for diffrent slope environments. However, this method is not applicable for the downslope walking since downslope walking trajectories vary greatly from those of upslope walking [21]. In an attempt to enable inclined walking, be it upslope or downslope, we conducted a study that used Principal Component Analysis (PCA) to generate the walking trajectories [22]. The results provided an avenue for performing real-time inclined walking using an information set of lower dimension [23]. However, this solution cannot avoid detecting the angle of inclination, which may pose some risks since the misdetection can cause a stability problem. Therefore, a new methodology should be considered, keeping in mind that the new technique would have to avoid detection of the slope angle and real-time heavy optimization.

1.1 AMPRO II

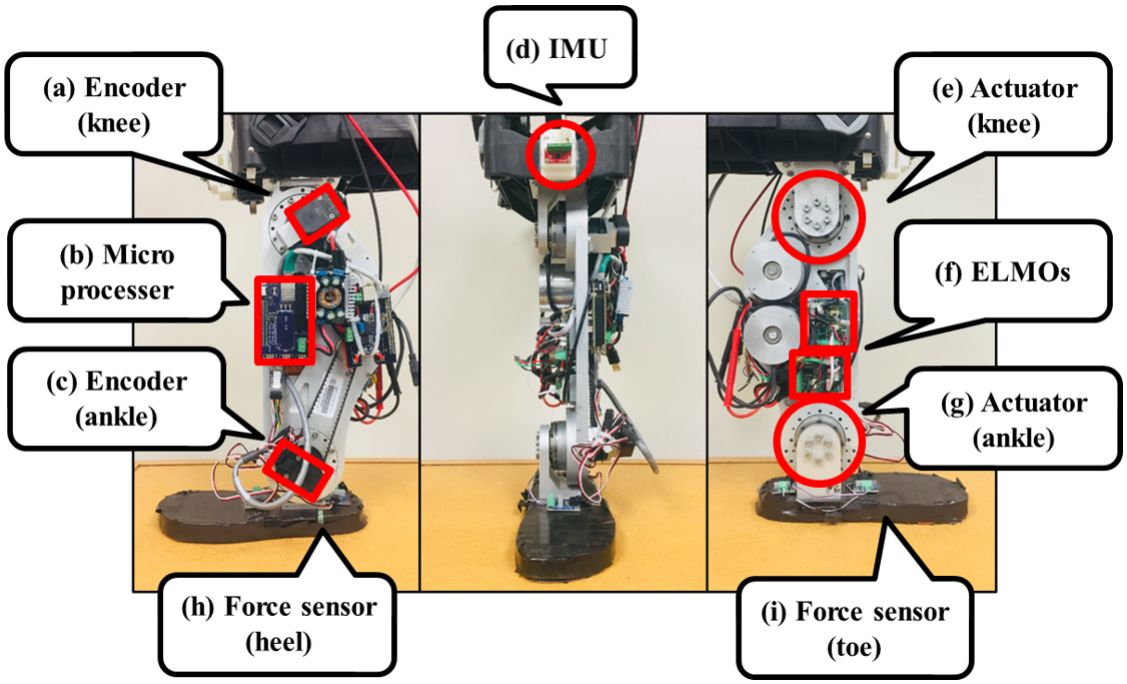

Figure 1.6: AMPRO II is the second version powered transfemoral prosthesis developed at Texas A&M University.

AMPRO II (A&M Prosthesis II) is the second generation powered transfemoral prosthetic system designed at Texas A&M University (Fig.1.6). It is fully actuated with two actuators on the ankle and knee, respectively (Fig.1.6 g,e). AMPRO II senses the user's walking progression and controls two actuators to follow the appropriate joint angle trajectories. A 9-axis Inertial Measurement Unit (IMU) on a L-shape adapter of the prosthesis (Fig.1.6 d) provides the thigh angle to calculate the state of user's gait progression. Depending on the walking progression the processor provides the desired torques to the ELMO drivers (Fig.1.6 f). Then, these motor drivers control two actuators on the ankle

and knee with the desired torques through Controller Area Network (CAN) protocol. During the gait cycle, two force sensors (FlexiForce) are used to detect the heel contact and the push-off for switching between the swing phase and the stance phase (Fig.1.6 h,i). For the processor and the high-level controller, two BeagleBone Blacks are used to calculate the gait progression and the proper state of walking gait, respectively in 200 Hz data rate (Fig.1.6 b). To perform human-like walking, we control the actuators on the ankle and knee to follow the human ankle and knee trajectories. Therefore, trajectory generation for the powered prosthesis is an essential procedure to design an appropriate controller that mimics human walking. Trajectories have to be generated for each gait cycle in real-time to produce stable, robust and human-like walking.

1.2 Thesis Structure

The flow of the thesis is described in this section. In the following Chapter 2, the main objective of the thesis is proposed before the idea is developed.

In Chapter 3, bio-mechanical traits of human walking on inclined surfaces are described by comparing the ankle and knee joint angle trajectories from 7 different slope conditions.

The control strategy for the prosthesis to mimic human walking trends is explained in Chapter 4. Chapter 4 consists of two different control strategies in two sections. First, an impedance controller is used for the stance phase with human impedance parameters. Second, a PD controller is utilized for the swing phase of gait cycle to follow joint angle trajectories which are generated by using Bezier polynomials.

In Chapter 5, the experiment protocol is proposed to verify the control strategies. Also, the experiment protocol is followed by the results of the experiments. The results, directly captured from the encoder on the prosthesis, are discussed by comparing a nominal human walking data and the joint angle trajectories from the device.

Additional improvements are also discussed in Chapter 6 to propose the next generation of the prosthesis as the future works.

The conclusion and discussion are presented in Chapter 7. The strength of the proposed framework is briefly summarized and concluded from the results in this chapter.

2. RESEARCH OBJECTIVES

The ability to walk on sloped surface is one of the most important functions for the transfemoral prosthesis. To provide appropriate prosthetic walking gait for various slopes, we characterized the human walking patterns on various slopes. Thus, this thesis focuses on generating human-like walking trajectories to perform sloped walking for a powered transfemoral prosthesis, without the former information of the slope in real-time.

3. HUMAN MOTION ANALYSIS FOR INCLINED WALKING

3.1 Human Data Analysis for Inclined Walking

People have their own strategy for different walking conditions. Even though individuals may have different characteristics, such as heights, limb lengths, and walking patterns, they all share common characteristics of walking [21] because of the kinematic traits of human. During normal walking, ankle and knee rotation will occur - also termed as dorsiflexion, plantar flexion for the ankle, and flexion, extension for the knee (Fig.3.1).

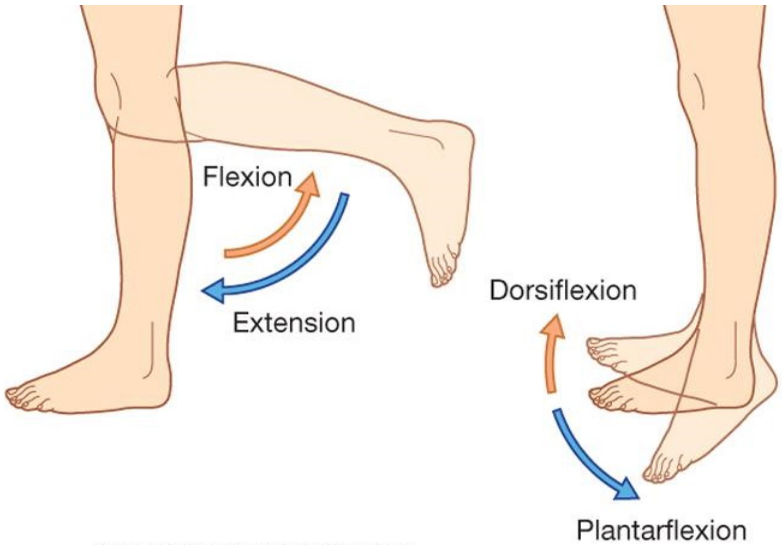

Figure 3.1: The knee joint rotates in two direction: flexion and extension, while the ankle joint moves in two directions: dorsiflexion and plantar flexion

3.1.1 Human walking data

To do a bio-mechanical analysis for human walking, we collected human walking data and joint trajectories for the ankle and knee joints with a motion capture system (9 Oqus

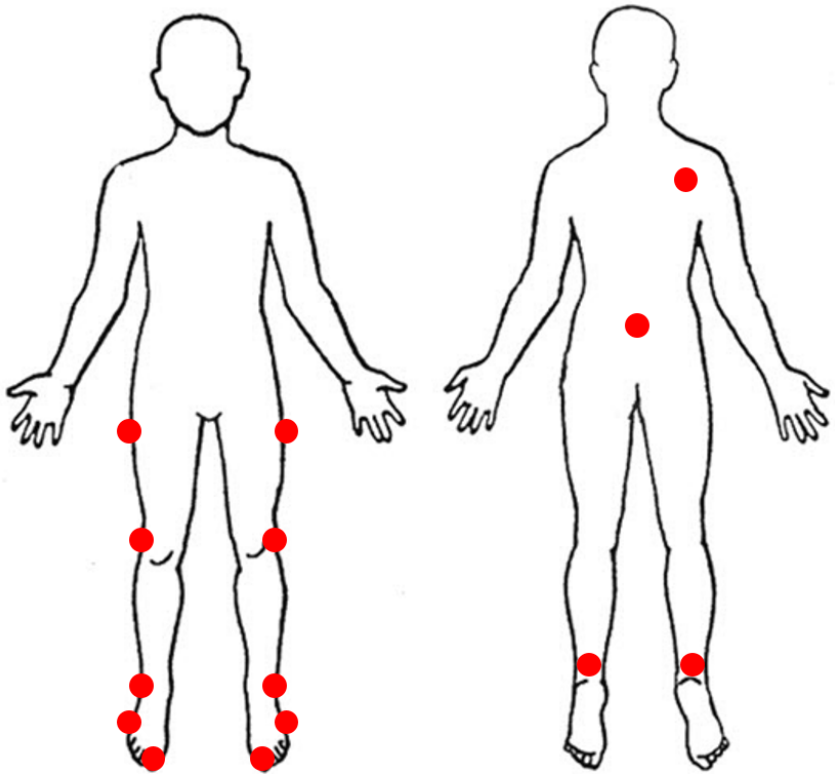

Figure 3.2: Bio-mechanical analysis for human walking can be done by utilizing camera-based motion capture system. (14 reflective markers were used)

210c cameras, Qualisys North America, Inc., Highland Park, Illinois, USA). We put 14 reflective markers on the body of a healthy young adult (male, 28 years, 5' 7" height, 150 lb weight) to capture the subject's joint trajectories while walking on a treadmill. The markers were put on the subject's right shoulder, hip, knee, ankle, heel, toe, toe bone and his left side of the back, hip, knee, ankle, heel, toe, toe bone. During the test, the inclination of the treadmill was varied by 7 different angles: -15°, -10°, -5°, 0°, 5°, 10°, and 15°. We specified the limit of the slope angle at $\pm 15°$ since angles exceeding $\pm 15°$ are rarely encountered in the daily living.

3.1.2 Flat-ground walking

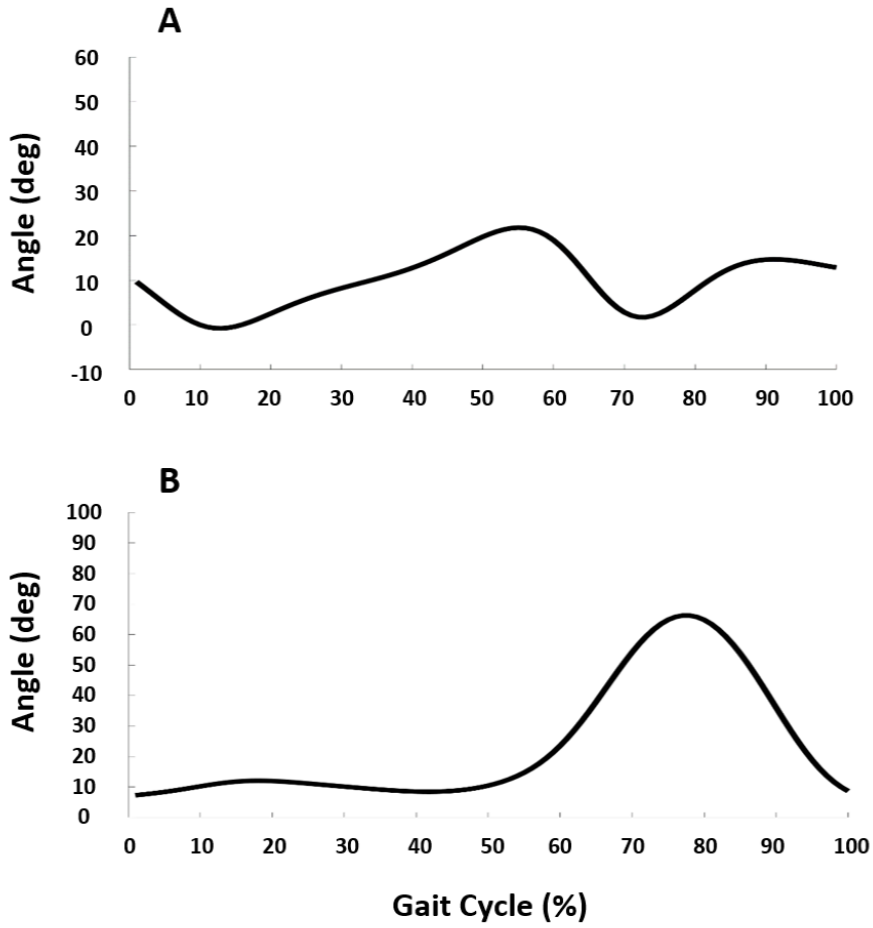

Figure 3.3: Joint angle trajectories for flat-ground walking (A: ankle joint angle, B: knee joint angle)

Since human walking is periodic, we focus on only one gait cycle of human walking. When illustrated, human walking trajectory is considered to consist of roughly two walking phases, called stance phase and swing phase; it can be divided into more subsections depending on the definition of subsections (e.g., Early-stance, Mid-stance, Late-stance,

Pre-swing, Mid-swing, Late-swing), but we consider only two sections in this research. The stance phase indicates the phase that lasts from heel contact to toe-off; during the stance phase, one of the legs is on the ground. On the other hand, the swing phase indicates the phase that the leg is in the air. Commonly, the stance phase is specified from 0% to 60% of the gait cycle, and the swing phase is specified as the rest of the gait cycle.

Human walking analysis is started from flat-ground walking because flat-ground is the most commonly faced terrain condition in our daily lives; thus we refer to flat-ground walking trajectory as the base-line. Since the prosthesis system that we used has two actuators, on the ankle and knee, we looked into the ankle and knee joint angles to describe flat-ground walking. For the ankle, it can be described by its rotating joint angle: dorsiflexion and plantar flexion. During human walking, the ankle undergoes dorsiflexion before heel strike and plantar flexion during push-off (Fig.3.3A). Likewise, the knee joint is also said to undergo angular deflections: slight flexion and extension after heel strike, and extensive flexion and extension during the swing phase (Fig.3.3B).

3.1.3 Upslope walking

Compared to the base-line, it is shown that upslope walking trajectories have a consistent patterns as the slopes are varied from 5° to 15°. The ankle joint angle trajectories indicated that the ankle joint angle increased, with respect to the slope increment, in the range of 0% – 45% and 80% – 100% of the gait cycle. On the other hand, in the mid range of the gait cycle, all ankle joint trajectories tended to merge into the base-line regardless of the slope angle (Fig.3.4A). An similar trend was observed in the knee joint angle trajectories (Fig.3.4B).

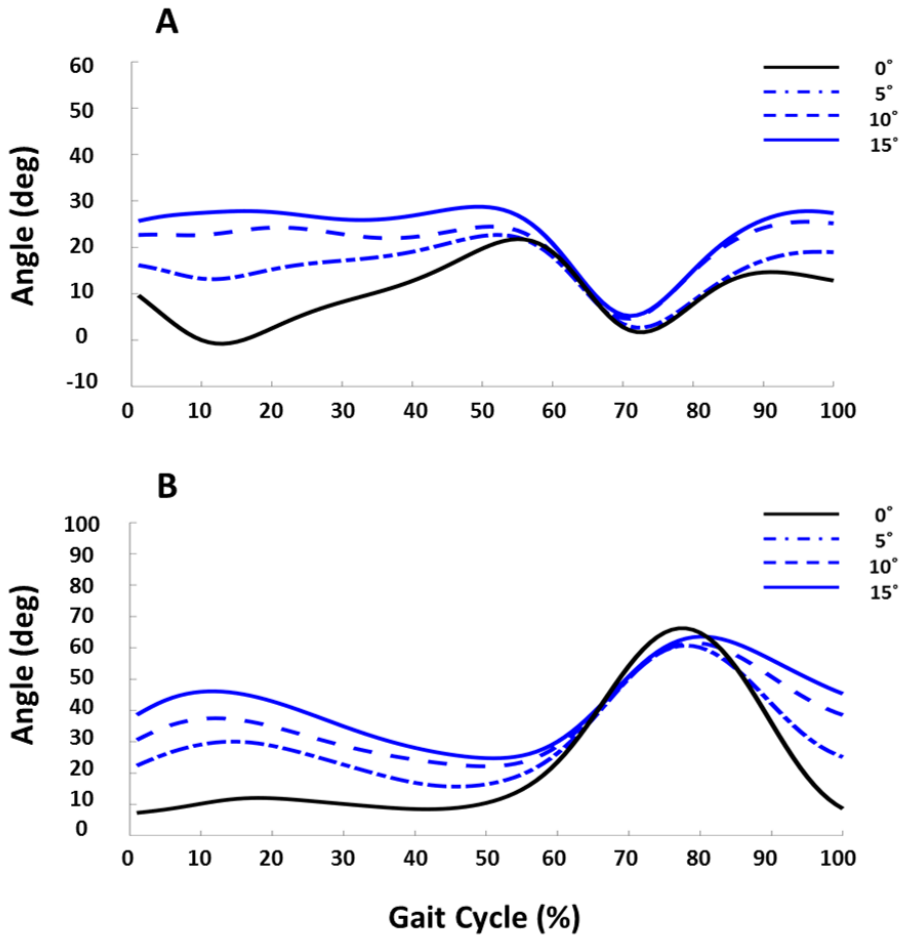

Figure 3.4: Joint angle trajectories for upslope walking compared to the flat-ground walking trajectory (0°, 5°, 10°, and 15°)
(A: ankle joint angle, B: knee joint angle)

3.1.4 Downslope walking

It was found that the walking pattern for the downslope was entirely different from that of upslope walking [21]. According to the data, when the subject walked on downslope surfaces, the ankle joint angle seemed to remain the same as the base-line regardless of the inclination angles (Fig.3.5A). On the other hand, for the knee joint angle, as the decline grew steeper, the deviation of the knee joint trajectory from the base-line became

significant (Fig.3.5B).

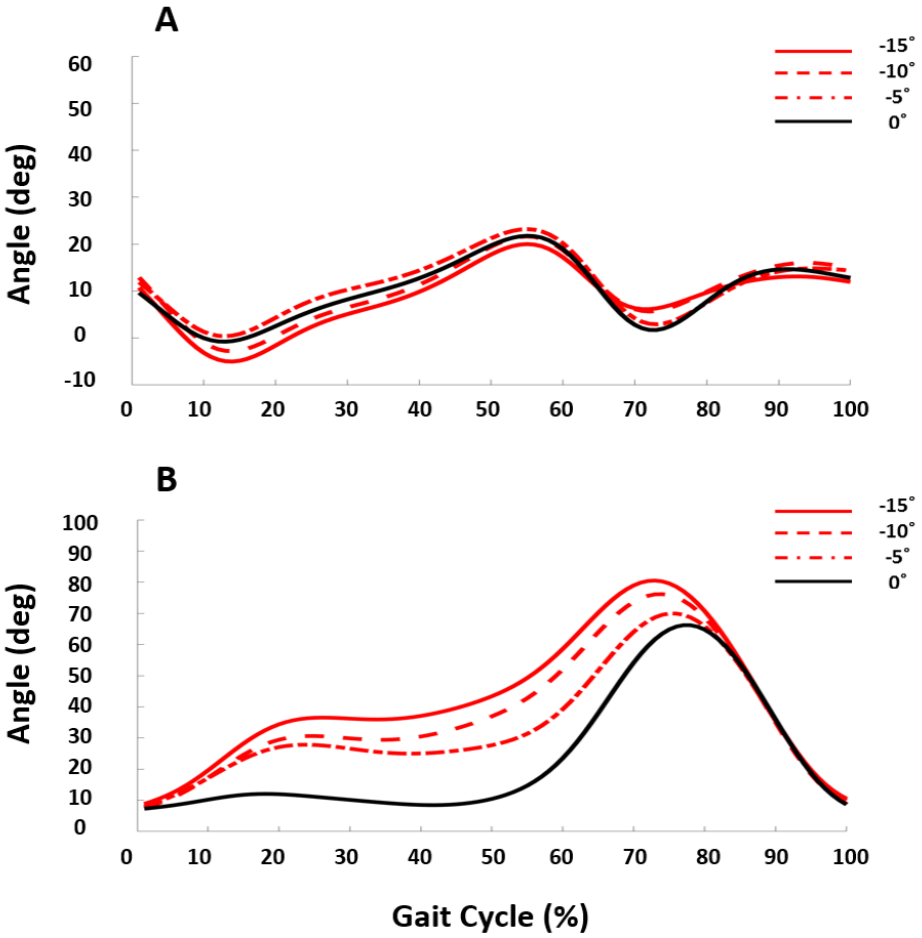

Figure 3.5: Joint angle trajectories for downslope walking compared to the flat-ground walking trajectory (-15°, -10°, -5°, and 0°)
(A: ankle joint angle, B: knee joint angle)

4.1 Prosthesis Strategy for Inclined Walking

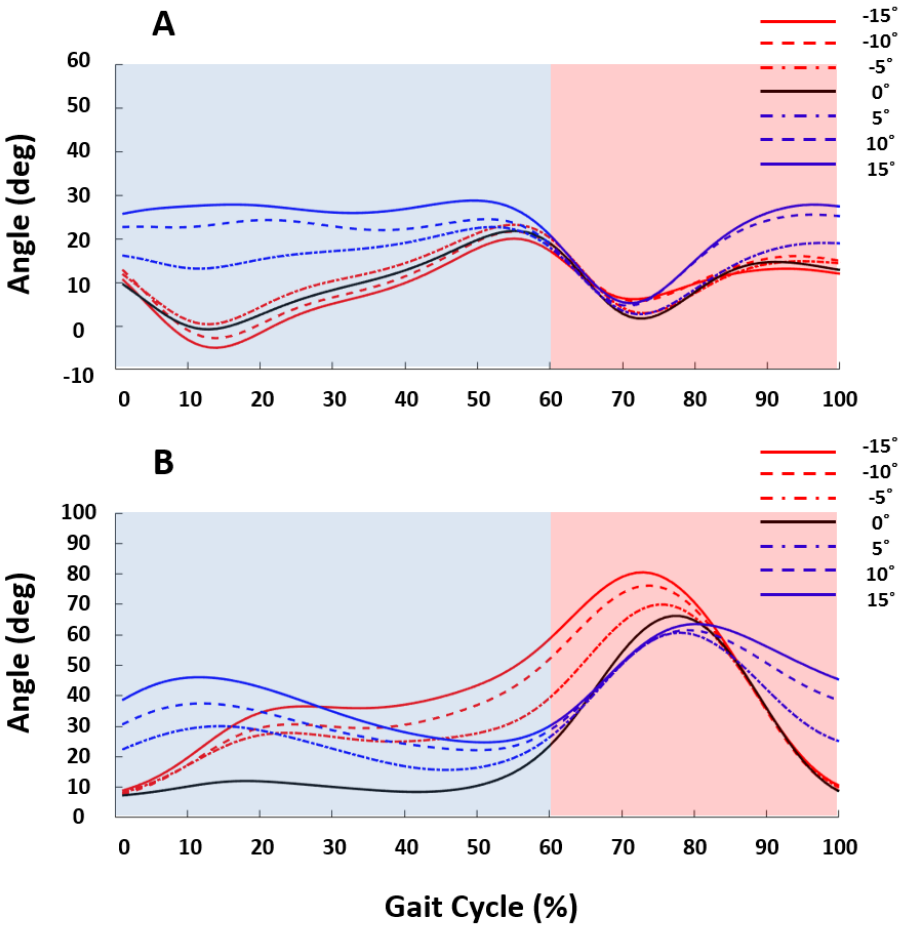

Figure 4.1: Two different strategies to the robotic system for inclined walking

In order to mimic the natural gait of humans on inclined surfaces, we apply two different methods to the robotic system (Fig.4.1): i) During the stance phase, the prosthesis is controlled using impedance parameters of the human subject, while ii) PD control is

implemented during the swing phase of the gait cycle. Low gain PD controller in the terminal swing phase makes the prosthesis adapt to the different terrains without any conflicts. During the early to mid swing phase (60% – 85%) of the gait cycle, upslope walking trajectories show that the ankle and knee joint angle trajectories conform to the base-line (Fig.4.1). On the contrary, at the same section of the gait cycle, the knee joint angle trajectories for downslope walking vary considerably with the inclination angle; if the knee flexion of the prosthesis is not enough while walking downslope, it could hit the slope. To generate the proper trajectories with respect to the inclination, Bezier curves are utilized during the early-mid swing phase; general PD controller is implemented to track the desired trajectory.

4.1.1 Stability of walking with prosthesis

4.1.1.1 Stability of the periodic orbit

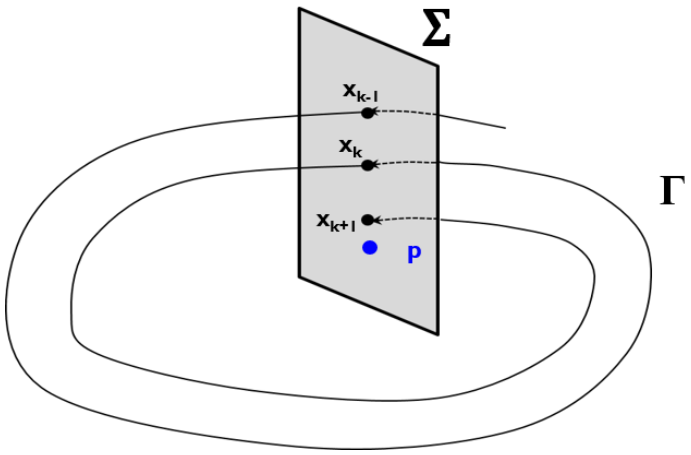

Figure 4.2: The basic concept of Poincare map

For the prosthesis, a stability problem should be carefully considered to avoid malfunction during user's walking. In the field of bipedal robotics and prostheses, the repetition

of movement (walking) is one criterion for assessing stability since it is periodic motion. To check the stability of these periodic movement, *Poincare map* (a.k.a. *the first return map*) is generally utilized. This map helps us to analyze a system which appears to have a periodic behavior.

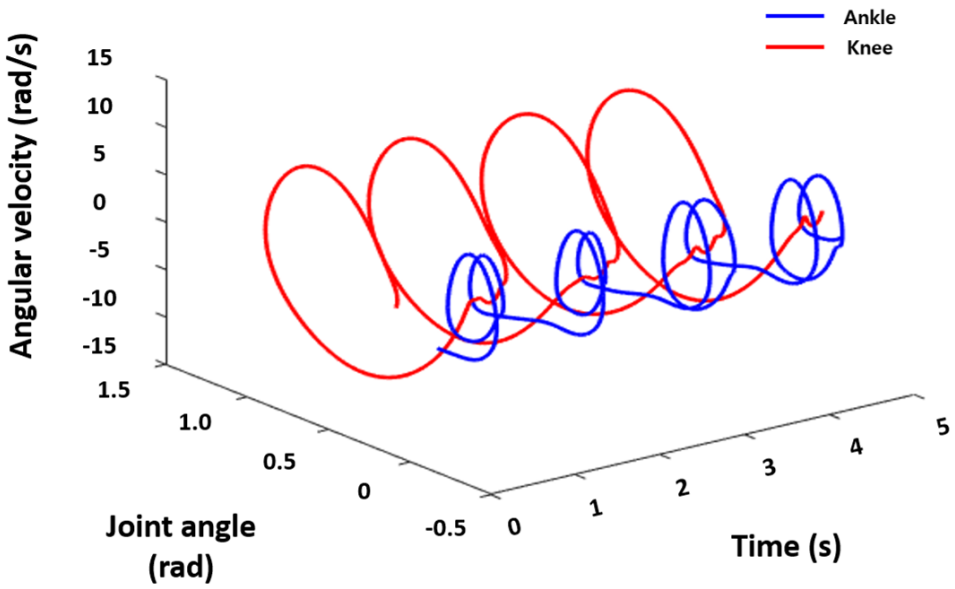

Figure 4.3: 3-Dimensional phase portrait during 4 steps of human on flat-ground

A phase portrait, which is a function of a state vector, is a geometric description of the trajectories of a dynamical system in the phase plane. From a phase portrait, we gain invaluable information of a dynamical system, such as the stability. Fig.4.3 indicates the phase portrait of 4 steps of human walking from an isometric perspective; the joint angle displacement and time are represented on the x-axis and the y-axis, respectively, and the angular velocity is indicated on the z-axis. It is shown that human walking has a periodic movement. When we check Fig.4.3 in the x-z plane, a remarkable periodic trend is observed (Fig.4.4). From Fig.4.4, we can construct a section Σ, transverse to the corre-

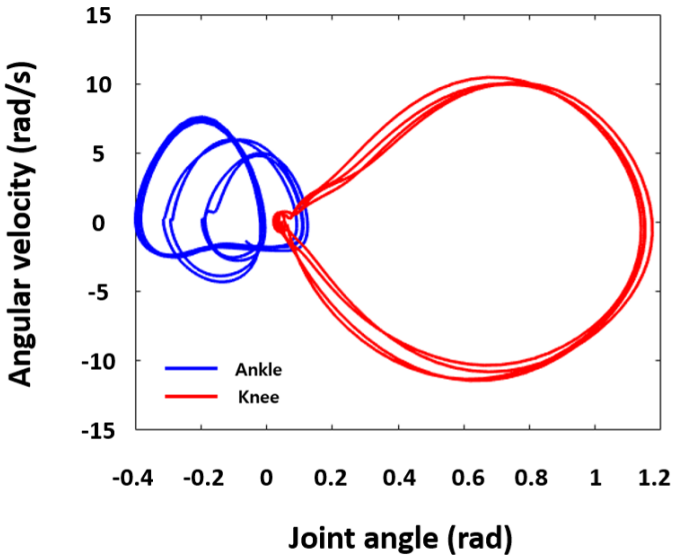

Figure 4.4: 2-Dimensional phase portrait during 4 steps of human on flat-ground

sponding closed orbit Γ, to see the discrete trend on the surface (Fig.4.5). An orbit starting at $x_0 \in \Sigma$ reaches Σ again when it is following the phase flow. When an orbit passes a section Σ, a point (x_k) is created on the surface. The *Poincare map* $P : U \subset \Sigma \to \Sigma$ is defined by

$$x_{k+1} = P(x_k) \tag{4.1}$$

If x_{k+1} converges to a fixed point p, it stays on the limit cycle:

$$p = P(p) \tag{4.2}$$

After we get a limit cycle, we should check the stability of a limit cycle $P(p+\epsilon)$. Since it is close enough to the limit cycle (ϵ is extremely small), Taylor expansion can be used to approximate the map.

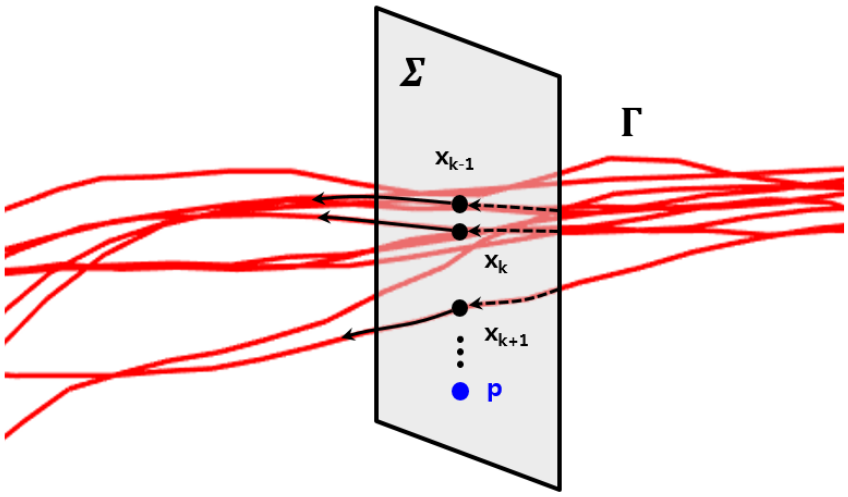

Figure 4.5: Poincare map is constructed in the phase portrait of human walking gait cycle.

$$P(p+\epsilon) = P(p) + DP|_p\epsilon \tag{4.3}$$

Since it is on the limit cycle, $Eq.4.3$ can be re-described with a fixed point p:

$$P(p+\epsilon) = p + DP|_p\epsilon \tag{4.4}$$

We only care about the size of derivative term in comparison to the size of ϵ to check whether it diverged or converged. By checking the eigenvalues of $DP|_p\epsilon$, which refers to *the Floquet Multiplier*, the stability of the limit cycle is confirmed. If only one eigenvalue is equal to 1 and other eigenvalues are less than 1, then the system is stable. On the contrary, if at least one eigenvalue is larger than 1, the system is diverged, which means it

is unstable.

4.1.1.2 Human-inspired control

In the field of robotics and prostheses, to guarantee the system which appears a repititive behavior, e.g. walking, a framework based on Hybrid Zero Dynamics (HZD) was proposed, called human-inspired control [18], [24]. HZD approach describes human walking functions in a mathematical way by using human data as the reference [25], [26]. These nominal human walking functions can be generated from non-linear optimization problems which make them mathematically stable functions. By tracking these functions using feedback control method, the system can be called a stable system.

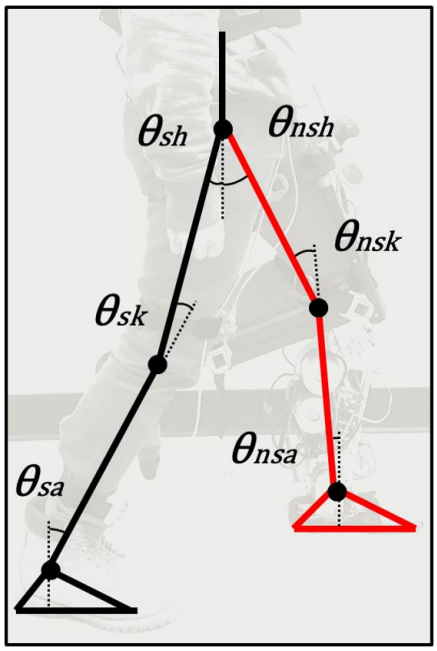

Figure 4.6: 7-link bipedal robotic model which is inspired from human [6]

To start with the human-inspired control, 7-link anthropomorphic bipedal robotic model is utilized to represent human walking. The coordinates of the model is based on the hu-

man subject as $\theta = [\theta_{sa}, \theta_{sk}, \theta_{sh}, \theta_{nsh}, \theta_{nsk}, \theta_{nsa}]^T \in Q_R$, where Q_R is the configuration space, a submanifold of R^6 (Fig.4.6).

During human walking, in contrast with the continuous dynamics of human walking, a discrete event happens when the heel contact occurs and this impact affects the system with an instant change of joint velocities [26]. In consideration of both the continuous dynamics of walking and the discrete impact at heel contact, the bipedal robotic system is regarded as a hybrid system [26]. The continuous dynamics of the system is described in the equation of motion using the Euler-Lagrange formula:

$$D(\theta)\ddot{\theta} + C(\theta)\dot{\theta} + G(\theta) = Bu \tag{4.5}$$

where, $D(\theta)$ is the inertial matrix, $C(\theta)$ indicates the Coriolis term, and $G(\theta)$ is the gravity vector, the gradient of the potential energy. Since 6-coordinate robotic model is assumed to be fully actuated, B is the 6-dimensional identity matrix and the input of the system is the torque u. An affine control system $\dot{x} = f(x) + g(x)u$ can be represented by re-describing $Eq.4.5$ in state variable $x = (\theta, \dot{\theta})^T$.

In order to mimic the human walking, human-like walking trajectories, called Canonical Walking Functions (CWF), were obtained from the walking data of several subjects [18]. They conducted 6 different canonical walking functions considering the 7-link model with flat foot assumption: δp_{hip} the linearized hip position, θ_{sk} the stance knee, θ_{nsk} the non-stance knee, δm_{nsl} the non-stance slope, θ_{tor} the torso angle, and θ_{nsf} the non-stance foot [19]. These canonical walking functions have two different types of desired outputs: the linearized hip velocity ($y_1^d(\theta, \dot{\theta})$), and the solution of a second order system ($y_2^d(\theta, \dot{\theta})$) ($d$ refers to the desired value).

$$y_1^d(\theta, \dot{\theta}) = \delta \dot{p_{hip}}(\theta, \dot{\theta}) \tag{4.6}$$

$$y_2^d(\theta, \dot{\theta}) = \begin{bmatrix} \theta_{sk} & \theta_{nsk} & \delta m_{nsl} & \theta_{tor} & \theta_{nsf} \end{bmatrix}^T \tag{4.7}$$

Each output $y^d(t, \alpha)$ can be described as the exponential function depending a set of parameter α; a set of α represents the characteristic of each canonical walking function. Note that v_{hip} is a member of α as well.

$$y_1^d(t) = v_{hip} t \tag{4.8}$$

$$y_2^{d,i}(t, \alpha) = e^{-\alpha_1 t}(\alpha_2 cos(\alpha_3 t) + \alpha_4 sin(\alpha_3 t)) + \alpha_5 \tag{4.9}$$

where, $i \in \theta_{sk}$, θ_{nsk}, δm_{nsl}, θ_{tor}, θ_{nsf}

$$y(\theta, \dot{\theta}, \alpha) = \begin{bmatrix} y_1(\theta, \dot{\theta}) \\ y_2(\theta, \alpha) \end{bmatrix} = \begin{bmatrix} y_1^a(\theta, \dot{\theta}) - v_{hip} \\ y_2^a(\theta) - y_2^d(\rho(\theta), \alpha) \end{bmatrix} \tag{4.10}$$

where, $y_1(\theta, \dot{\theta})$ is the relative degree one output, and $y_2(\theta, \alpha)$ is the relative degree two output. These outputs refers to the differences between the actual ($y_1^a(\theta, \dot{\theta})$, $y_2^a(\theta)$) and the desired (v_{hip}, $y_2^d(\rho(\theta), \alpha)$) canonical walking functions ($Eq.4.10$). $\rho(\theta)$ indicates the phase variable to make the system as the state based system, which is independent of time. $\rho(\theta)$ can be parametrized by using the linearized hip position (δp_{hip}), its initial value (δp_{hip}^{init}), and the desired hip velocity (v_{hip}): $\rho(\theta) = (\delta p_{hip} - \delta p_{hip}^{init})/v_{hip}$. If these outputs ($y_1(\theta, \dot{\theta}), y_2(\theta, \alpha)$) are driven to zero, the robotic system will perform a human-like walking. However, even though the system is stably controlled in the continuous dynamics, the stability problem should be ensured in a discrete event as well. Therefore, HZD surface is considered in this situation.

$$Z_\alpha = (\theta, \dot{\theta}) \in TQ_R : y_1(\theta, \dot{\theta}) = 0, y_2(\theta, \alpha) = 0, L_{fy2}(\theta, \dot{\theta}, \alpha) = 0 \tag{4.11}$$

where, TQ_R is the tangent bundle of the system and $L_f(\theta, \dot{\theta}, \alpha)$ represents the lie derivative.

When the outputs of the system are driven to 0, the HZD surface can be derived as ($Eq.4.11$). Since this surface is an invariant set, the outputs stay at 0 for the continuous dynamics. When an impact occurs at the heel contact, the system is affected by the impact; intense velocity jumps occur at the joints. Thus, the relaxed constraints can be considered to the HZD surfaces, called Partial Hybrid Zero Dynamics (PHZD) surface ($Eq.4.12$).

$$PZ_\alpha = (\theta, \dot{\theta}) \in TQ_R : y_2(\theta, \alpha) = 0, L_{fy2}(\theta, \dot{\theta}, \alpha) = 0 \tag{4.12}$$

From $Eq.4.12$, it is shown that the constraint of the hip velocity $(y_1(\theta, \dot{\theta}))$ is relaxed in PHZD surface. This allows the system adjust the hip velocity after an impact for compensating the intense effect of the impact. However, this can affect the system to stray from the PHZD surface. In order to make the system stay in an invariant set under the impact, the PHZD constraint is considered ($Eq.4.13$).

$$\triangle(S \cap PZ_\alpha) = PZ_\alpha \tag{4.13}$$

With the PHZD constraints, the system does not stray from the PHZD surface PZ_α under the impact $\triangle$ (reset map) when the system is in the switching surface S in the PHZD surface. By providing joint angle trajectories which satisfy PHZD constraints, they make the system stay stable during the operation. However, in order to find α sets for generating stable joint angle trajectories, the optimization problem should be solved; this can be demanding for the system to generate the trajectories in real-time.

4.1.1.3 Stability of human walking

Thus, in this framework, we decided to use human walking trajectories directly rather than generating mathematically stable walking trajectories. Though the inherent stable nature of the human gait remains a puzzle to this date, it is widely accepted that humans are more robust than robots. There is no exact metric to measure and verify the stability of human walking in a systemic way because human walking is overly complicated and humans are hard to model. However, what we can say confidently about human walking is that human walking is stable, well-balanced and repetitive; humans have the ability to react to unexpected situations including the external force when the heel impact happens. Humans can withstand perturbations within reasonable limits and can continue walking as before the perturbations. Furthermore, by using low gain PD control before the heel contact, the affect of an impact at the heel contact can be compromised.

4.1.2 Synchronization of step progression

In order to achieve the interaction between the robotic system and the user for a stable walking, it is crucial to synchronize the user's kinematics during the gait cycle; such synchronization would enable the detection of the user's walking progression and provide the appropriate control signal to follow the right track. To achieve this goal, a phase variable has been widely proposed and utilized in the field of robotics [17] – [20], [24] – [27]. A phase variable is a variable which parameterizes the phase of human locomotion. Villarreal *et al.* investigated multiple phase variable candidates related to the hip angle with respect to a global coordinate frame [28]. According to the study of phase variable, the chosen phase variable must be monotonic; i.e. it should be linearly mapped to the walking gait cycle in a one-to-one manner. In our previous study, we used the hip position as a phase variable [6]. However, to calculate the hip position, we need two different joint kinematics – thigh and shank joint angles. To obtain the necessary data, we would have

to mount two IMUs at the thigh and the shank. Such mountings make it inefficient for the users to use because it would interfere with the daily activities of the user. Hence, it is required to minimize our reliance on sensors on user's body. Also, the hip position cannot adapt to walking speed precisely. Therefore, there is a need for an alternative phase variable to perform the inclined walking more actively; we decided to use the thigh angle in a global coordinate frame as the phase variable. The global thigh angle has been shown to be a good candidate [29], and by using the thigh angle as a phase variable, we were able to put an IMU on the prosthesis and removed all the sensors from the user's abled leg (Fig.4.7).

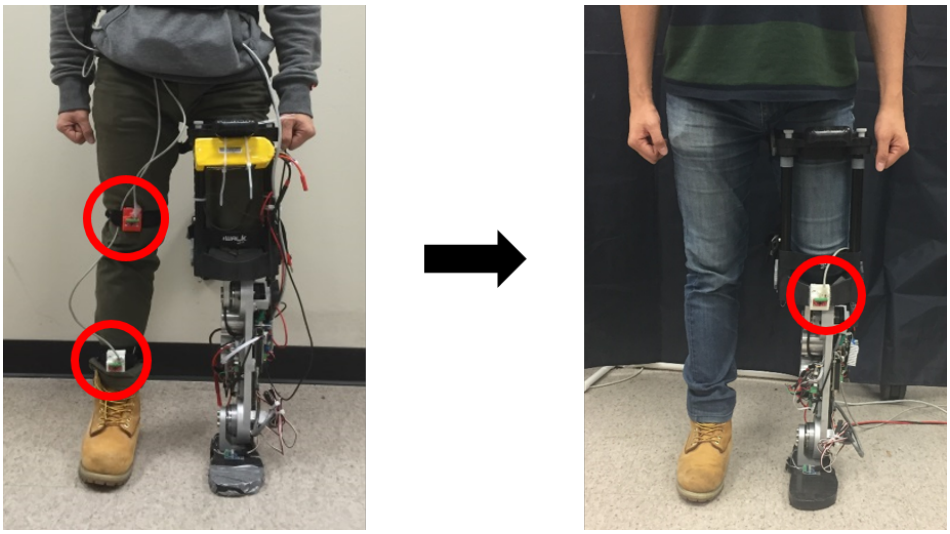

Figure 4.7: The change of IMU sensor position can provide more practical usage of the prosthesis to the users.

According to the previous research [29], the change of the global thigh angle can be assumed to be a consistent function that has the same periodicity as the human walking gait cycle (Fig.4.8). Therefore, it enables accurate detection of the stage of the gait cycle without having to consider the time that has elapsed. Since the thigh angle under consid-

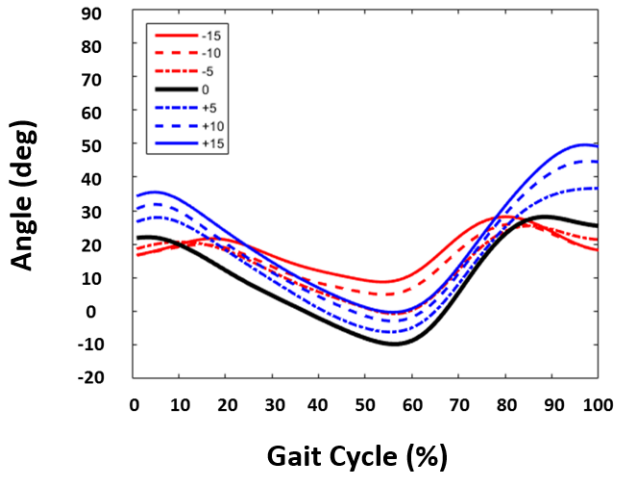

Figure 4.8: The movement of a global thigh angle during a gait cycle on the sloped surfaces

eration is that of the amputated leg, the operation of the prosthesis is independent of the status of the intact leg – allowing the user to have complete and independent control over the prosthesis' action.

In order to use the thigh angle as the phase variable, it should be linearized. Further, to satisfy the condition for its monotonic trend (which the thigh angle by itself fails to meet (Fig.4.8)) the monotonic relationship between the thigh angle and its derivative or integral (Fig.4.9) is considered as the phase variable [29]. Between its derivative and integral, the latter is chosen because it is less noisy. Before using the thigh angle to compute the phase variable, a normalization process is needed (the variation of the phase variable from 0 to 1 would indicate the walking progression from 0% to 100%). However, the thigh angle's range is different for each step. Therefore, to make the phase variable vary within the desired 0 to 1 range (Fig.4.10), we propose to normalize the global thigh angle using the updated range from the most recent gait cycle. During the normalization process, the

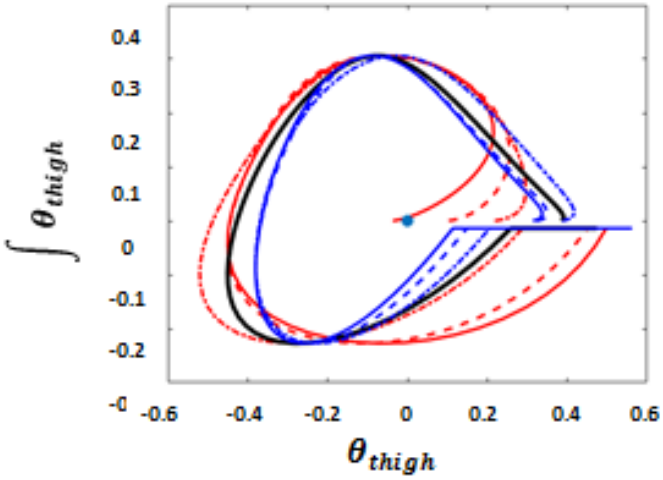

Figure 4.9: The relationship between the normalized thigh angle and its integral can be represented as a circular trend in quadrants.

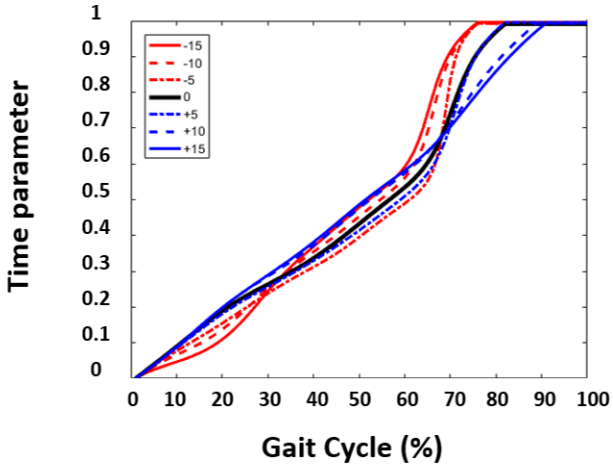

Figure 4.10: The phase variable from thigh angle is bounded in [0,1]

scaling factor is also updated as per the walking speed; it can be calculated in compliance with the duration of the most recent gait cycle. Using the phase variable calculated from

the global thigh angle along with two force sensors at the bottom of the prosthesis foot, the users will have complete authority over the operation of the prosthesis. However, since the thigh angle is not a perfect co-sine function, the calculated phase variable does not reach 1 at the exact 100% of the gait cycle. By ensuring the phase variable stays at the maximum value until heel contact occurs, the user can make a heel contact with the extended knee; this can be compromised by using low gain PD control for the late swing phase.

4.2 Impedance-Based Control

To successfully control the system during the stance phase, the impedance-based approach is suggested rather than trajectory tracking. Impedance control is broadly utilized in the field of robotics. Controlling the torque provides more flexibility for the users to interact with the system during operation [30], [31].

The torque at each joints can be described in series of passive impedance functions as follows:

$$\tau = k(\theta - \theta_{eq}) + b\dot{\theta} \tag{4.14}$$

According to the previous research [14], the mechanical impedance of human joints, the ankle and knee, varies while walking. In order to enforce this idea to the robotic system, researchers broke the human gait down into several states and assigned different constant impedance values to each state [14]. These states together are called a finite state machine (FSM), and their transitions are defined based upon biomechanical events, such as the movement of joint angles, heel contact, and push-off. A Piecewise Passive Impedance (PPI) controller with the proper impedance parameters was implemented for each state machine [4]. To emulate the biomechanical behaviors of a healthy human better, a Hybrid Impedance-Admittance (HIA) control framework was proposed [4]. In the HIA approach, they used the PPI controller for the early and mid stance phases of the gait cycle, and trajectory tracking for the rest of the gait cycle [4]. In addition, some researchers used

piece-wise functions to represent the ankle impedance during human walking gait cycle [32] – [33]. Rouse *et al.* estimated ankle impedance of humans during walking by using their customized robotic platform, called perturberator robot, which provides angular perturbation to the ankle's center of rotation during walking [34]. According to Lee *et al.*, the impedance parameters (the stiffness and damping) do not remain constant, especially, the stiffness linearly increases from heel contact to terminal stance phase, remaining low during entire swing phase [33].

The torque signals of each joint (τ_i) were computed from the model (i=0: ankle, i=1: knee), consisting of a virtual angular stiffness (k_i), damping parameter (b_i), and the equilibrium angle ($\theta_{eq,i}$) ($Eq.4.15$).

$$\tau_i = k_i(\theta_i - \theta_{eq,i}) + b_i\dot{\theta}_i \tag{4.15}$$

While the previous studies constrained the joint impedance parameters to be constant within a given state [14], [15], the impedance values used during the stance phase in this study, can be described as functions of the phase variable – the virtual angular stiffness (k_0, k_1) linearly increase with the phase varies, and the damping coefficients for the ankle and knee (b_0, b_1) are set to be constant. Even though the final equilibrium angles of the ankle and knee ($\theta_{eq,0}$, $\theta_{eq,1}$) were considered to decrease to -12° and -45° respectively during the swing phase according to [35], the equilibrium angles in this case were set to 0° and -5° since we used the impedance parameters only for the stance phase.

Base on the previous studies, we provided the varying impedance parameters, which can be represented by a function of time parameter from the phase variable (Fig.4.11). Exact values of the stiffness, damping, and equilibrium angles were chosen by combining the previous studies' data [4] – [15], [31] – [35].

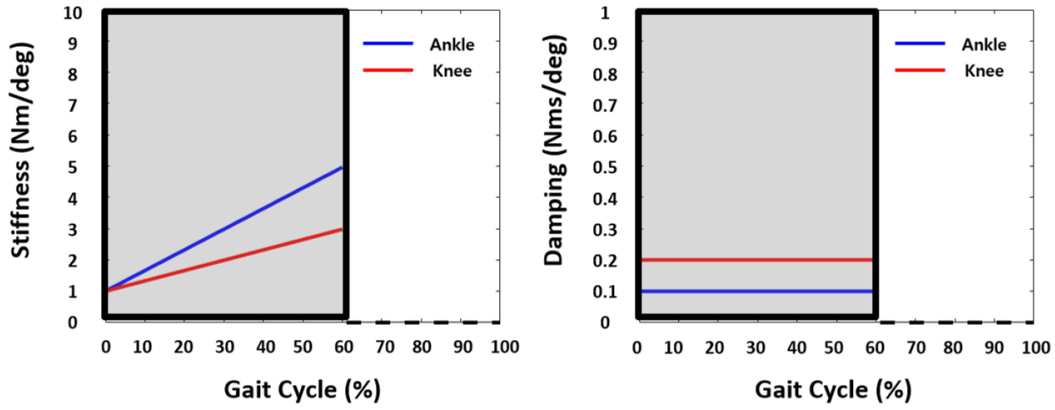

Figure 4.11: Varying impedance parameters, which is dependent on the time parameter from the phase variable

4.3 Cubic-Bezier-Polynomials-Based Optimization

During the swing phase, a different method should be considered to ensure sufficient foot clearance; especially downslope walking. Since the prosthesis is in the air during the swing phase, it is acceptable to use high impedance based controller for enough knee flexion while downslope walking. Therefore, we decided to use PD controller for trajectory tracking rather than using impedance controller; to generate the appropriate desired trajectories, we proposed to use Bezier polynomials. In order to have enough freedom to generate the curve, cubic Bezier polynomial ($Eq.4.16$) is chosen (Fig.4.12), where $t \in [0, 1]$.

$$Z(t) = (1-t)^3 P_0 + 3t(1-t)^2 P_1 + 3t^2(1-t)P_2 + t^3 P_3 \tag{4.16}$$

A Bezier curve is a parametric curve widely used in computer graphics related fields to generate the arbitrary curves with the finite points. Assuming n^{th} order Bezier curve, the curve consists of an initial control point (P_0), a final control point (P_n), and inner control points between P_0 and P_n; by moving these inner points, we can get any form of curve from a Bezier polynomial. The computational cost increases as the number of control

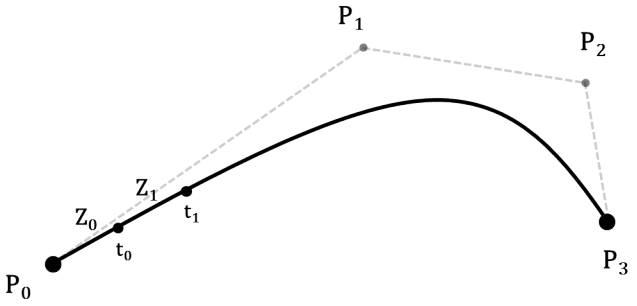

Figure 4.12: Using Bezier polynomials to generate the appropriate inclined walking trajectories

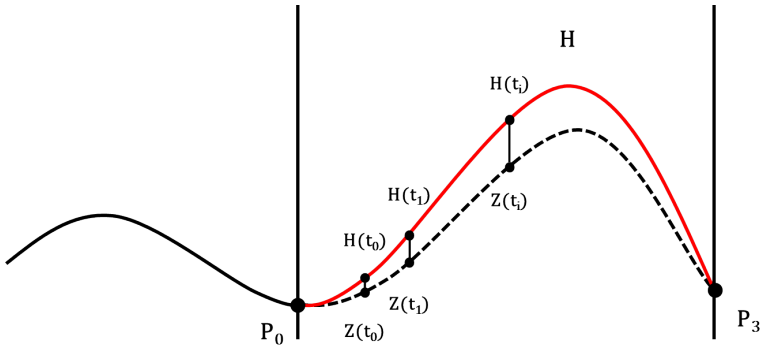

Figure 4.13: Bezier curve based optimization with human data (H)

points increases; thus it is important to choose the optimal number of control points to generate the desired trajectories.

Since the human walking trends of the ankle and knee are disparate, we set different parameters to generate the Bezier curve for the ankle and knee. For both the ankle and knee, the Bezier curve region is set from 60% to 85% of the gait cycle; the terminal swing phase (85% – 100%) is excluded in order to flexibly adapt to the upcoming terrain.

To obtain the parameters for generating the appropriate swing trajectories in real-time, an off-line optimization problem is solved with human data from the motion capture system. Initially, the starting point of the generated Bezier curve (P_0) is updated every single

gait cycle to generate a proper trajectory; this lets us newly generate suitable trajectories in accordance with the inclination. Also, the end point of the Bezier curve (P_3) is selected to be the point at which the current trajectory blends into the base-line trajectory (H). These following two conditions are required as the constraints in order to guarantee the continuity of the optimized trajectories.

$$Z(0) = P_0 \tag{4.17}$$

$$Z(1) = P_3 \tag{4.18}$$

Also, to guarantee the smoothness of the trajectories, the following equality constraints of the angular velocities should be considered:

$$\dot{Z}(0) = \dot{H}(P_0) \tag{4.19}$$

$$\dot{Z}(1) = \dot{H}(P_3) \tag{4.20}$$

To obtain a closer trajectory to the reference path H, it is necessary to have an objective function based on the distance between the Bezier curve and H (Fig.4.13) while satisfying the constraints ($Eq.4.17 - Eq.4.20$); 2-norm is used to find the optimal values.

$$min||Z(t) - H|| \tag{4.21}$$

$$s.t\ \ (Eq.4.17) - (Eq.4.20)$$

P_1, P_2 can be approximated by P_0, P_3 and their angular velocities (Fig.4.14) can be determined from the smoothness constraints ($Eq.4.22, Eq.4.23$).

$$P_1 = (P_0 + \overline{P_0 P_{1_x}} v_0) \tag{4.22}$$

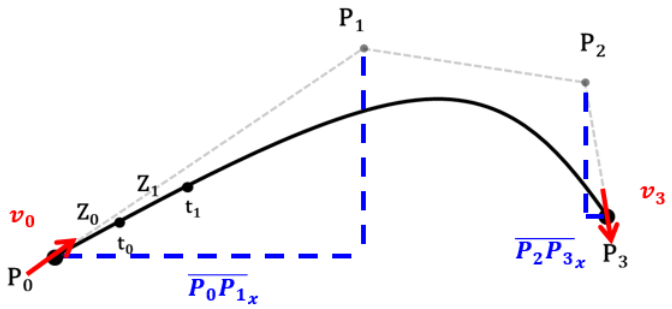

Figure 4.14: Re-describing P_1, P_2 by considering the smoothness constraints

$$P_2 = (P_3 - \overline{P_2P_{3x}}v_3) \tag{4.23}$$

where,

$\overline{P_0P_{1x}}$: the length of projection $\overrightarrow{P_0P_1}$ to x-axis

$\overline{P_2P_{3x}}$: the length of projection $\overrightarrow{P_2P_3}$ to x-axis

v_0: angular velocity at 60% of gait cycle

v_3: angular velocity at 85% of gait cycle

Thus, $Eq.4.16$ is described with P_0 and P_3, which can be transformed into the matrix form:

$$Z(t) = \begin{bmatrix} t^3 \\ t^2 \\ t \\ 1 \end{bmatrix}^T \begin{bmatrix} 2 & -2 & 3v_0 & 3v_3 \\ -3 & 3 & -6v_0 & -3v_3 \\ 0 & 0 & 3v_0 & 0 \\ 1 & 0 & 0 & 0 \end{bmatrix} \begin{bmatrix} P_0 \\ P_3 \\ \overline{P_0P_{1x}} \\ \overline{P_2P_{3x}} \end{bmatrix} \tag{4.24}$$

For the closer look, the objective function can be expressed with N set of way points as follows:

$$Z_i(t_i) = \begin{bmatrix} t_i^3 \\ t_i^2 \\ t_i \\ 1 \end{bmatrix}^T \begin{bmatrix} 2 & -2 & 3v_0 & 3v_3 \\ -3 & 3 & -6v_0 & -3v_3 \\ 0 & 0 & 3v_0 & 0 \\ 1 & 0 & 0 & 0 \end{bmatrix} \begin{bmatrix} x_0 \\ x_1 \\ x_2 \\ x_3 \end{bmatrix} = T_i B X \tag{4.25}$$

where,

$$i \in [1, N], T_i = \begin{bmatrix} t_i^3 & t_i^2 & t_i & 1 \end{bmatrix}, X = \begin{bmatrix} x_0 & x_1 & x_2 & x_3 \end{bmatrix}^T$$

Then, all values at the way-points can be represented as follows:

$$Z = TBX \tag{4.26}$$

Since the smoothness constraints are already satisfied by the re-described Bezier polynomials ($Eq.4.24$), only the continuity constraints should be considered. The continuity constraints ($Eq.4.17, Eq.4.18$) can be represented in a matrix form:

$$AX = C \tag{4.27}$$

where,

$$A = \begin{bmatrix} 1 & 0 & 0 & 0 \\ 0 & 1 & 0 & 0 \end{bmatrix}, X = \begin{bmatrix} x_0 \\ x_1 \\ x_2 \\ x_3 \end{bmatrix}, C = \begin{bmatrix} P_0 \\ P_3 \end{bmatrix}$$

To find the analytic solution of the equality constrained optimization problem, the problem is written as:

$$min||TBX - H|| \tag{4.28}$$

$$s.tAX = C$$

First, we could check whether the objective function f has a global minimum or not:

$$f = (TBX)^T TBX - 2H^T TBX + H^T H \tag{4.29}$$

$$\nabla_X f = 2(TB)^T TBX - 2(TB)^T H \tag{4.30}$$

$$\nabla_X^2 f = 2(TB)^T TB \tag{4.31}$$

Since the Hessian matrix of f ($Eq.4.31$) is positive definite, a global minimum exists. To find this minimum value, we used the Lagrangian Multiplier Method; this method lets us turn a constrained optimization problem into an unconstrained problem. The Lagrangian is:

$$L(X, \nu) = (TBX)^T TBX - 2H^T TBX + H^T H + \nu^T (AX - C) \tag{4.32}$$

To minimize L over X, set the gradient equal to 0:

$$\nabla_X L(X, \nu) = 2(TB)^T TBX - 2(TB)^T H + A^T \nu = 0 \tag{4.33}$$

$$\nabla_\nu L(X, \nu) = AX - C = 0 \tag{4.34}$$

It is expressed as a linear equation in matrix form:

$$\begin{bmatrix} 2(TB)^T TB & A^T \\ A & 0 \end{bmatrix} \begin{bmatrix} X \\ \nu \end{bmatrix} = \begin{bmatrix} 2(TB)^T H \\ C \end{bmatrix} \tag{4.35}$$

This linear equation ($Eq.4.35$) can be handled in the robotic system using C++. Since this is an off-line optimization problem, the system is only tasked with determining the Bezier curve polynomials using the angle values (P_0, P_3) and their angular velocity values ($\dot{P_0}$, $\dot{P_3}$). The off-line optimization problem was solved using MATLAB.

Also during the late swing phase, we suggested a low gain PD control to adapt to the unexpected terrain at heel strike. The rationale behind our choice of low gain PD controller over impedance controller is to make the knee extend fully and contact ground stably during the late swing phase. This makes the device more flexible and mimics the nature of a low gain passive device.

5.1 Bezier-Polynomials-Based Optimization Results

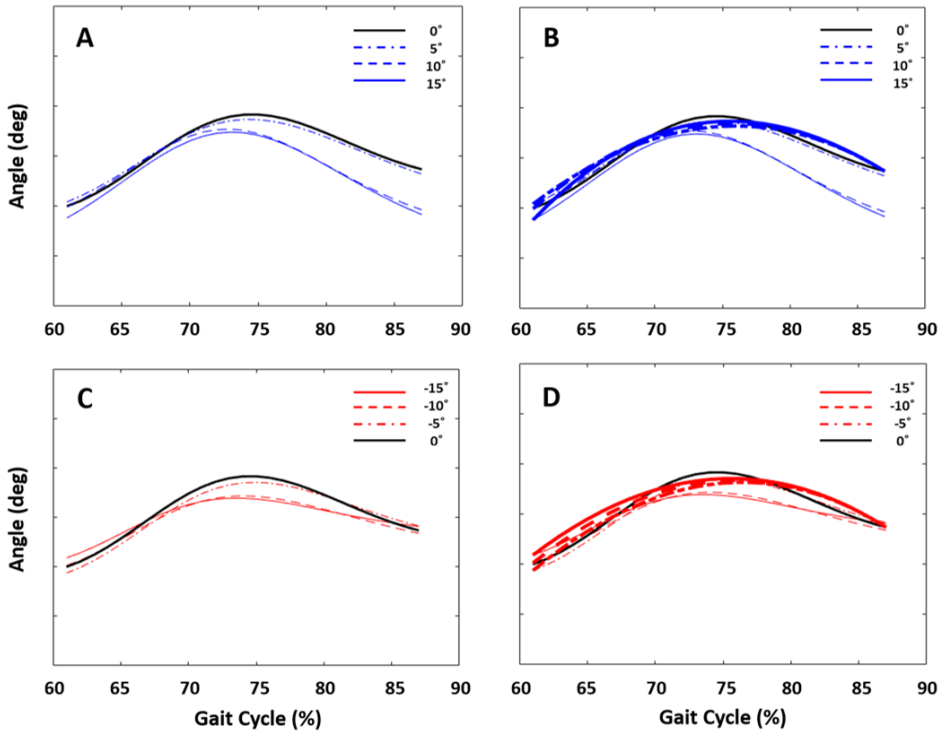

Figure 5.1: Comparison between human ankle data and the results of Bezier based optimization problem
A: Ankle angle trajectories on 0° – 15° slopes in 60%–85% of a gait cycle
B: Plot A with the generated trajectories from the optimization results
C: Ankle angle trajectories on -15° – 0° slopes in 60%–85% of a gait cycle
D: Plot C with the generated trajectories from the optimization results

To successfully perform inclined walking, the desired trajectories should be generated properly in accordance with human walking trends. During the swing phase, especially from 60% to 85% of the gait cycle, the desired trajectories were generated with off-line

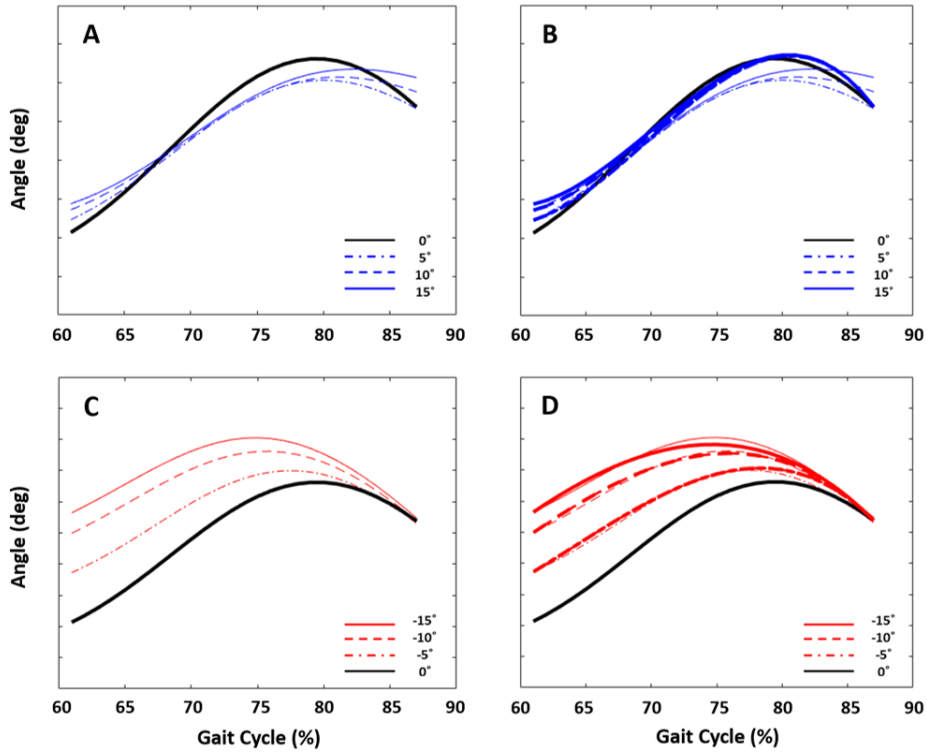

Figure 5.2: Comparison between human knee data and the results of Bezier based optimization problem
A: Knee angle trajectories on 0° – 15° slopes in 60%–85% of a gait cycle
B: Plot A with the generated trajectories from the optimization results
C: Knee angle trajectories on -15° – 0° slopes in 60%–85% of a gait cycle
D: Plot C with the generated trajectories from the optimization results

optimization problem using human data. The results of the off-line optimization problem are shown in Fig.5.1, Fig.5.2.

From the results in Fig.5.1, Fig.5.2, it is shown that the optimized trajectories (bold trajectories) are close to the human base-line trajectories. For the ankle joint angle, the Bezier polynomial is defined to merge into the level-walking trajectory regardless of the inclination angle (Fig.5.1B,D). For downslope walking, the generated trajectories resemble the human walking data corresponding to the same slope inclination (Fig.5.2D). During the upslope walking, the trend of the knee joint angle blends to the base-line, similar to the

ankle joint movement (Fig.5.2B). The controller is designed to track these desired trajectories during the swing phase to make the prosthesis perform appropriately for the inclined surfaces.

5.2 Experimental Set-up & Protocol

To validate that the system successfully meets the needs for inclined walking, we designed an indoor experiment using a treadmill. The experimental protocol was reviewed and approved by the Institutional Review Board (IRB) at Texas A&M University.

5.2.1 Indoor experiment protocol

The indoor experiment was performed on a treadmill at five different slopes: -10°, -5°, 0°, 5°, and 10°. Each walking trial was conducted at a treadmill speed based on the subject's comfort (1.06 mph) and the encoder data from the prosthesis was recorded to check its performance.

5.3 Experimental Results

The prosthetic walking data from the encoders and the human walking data from IMUs on the intact leg were compared in order to verify whether the prosthesis mimics human walking. For both the ankle and knee, the human walking data from the IMUs during the test differed from the trends captured from the motion capture system (Fig.3.3 – Fig.3.5).

For the ankle joint angle (Fig.5.3A – Fig.5.7A), it is commonly shown that the push-off is small compared to the human walking trends since the current platform has a rigid foot. Also, since the phase variable met the maximum value earlier than 100% of a gait cycle, the push-off timing was different from human walking trends. Especially, for the flat-ground walking (Fig.5.5A), a difference between the ankle encoder and ankle joint angle from IMUs was shown in the mid-range of a gait cycle. According to the encoder data, a dorsiflexion angle is large during the late stance phase; low stiffness might affect the ankle

and hinder the push-off appropriately. It is also commonly shown from all results that a slight knee flexion and extension did not happen during the stance phase for the prosthesis (Fig.5.3B – Fig.5.7B). This is because the subject tends to make a heel contact with a fully extended knee for safe weight-shift. Also, a maximum knee flexion is restricted to 1.1 radians because of the hardware limitation.

The controlled behaviors of the prosthesis in 5 different slopes are shown in Fig.5.8 – Fig.5.12. These figures were captured for one gait cycle, from heel strike to another heel strike. Fig.5.8, Fig.5.9 represents the downslope walking on tilted treadmill with an inclination of -10° and -5°, respectively. In addition, Fig.5.10 represents the flat-ground walking on the treadmill. The upslope walking with an inclination of 5° and 10° are indicated in Fig.5.11, Fig.5.12.

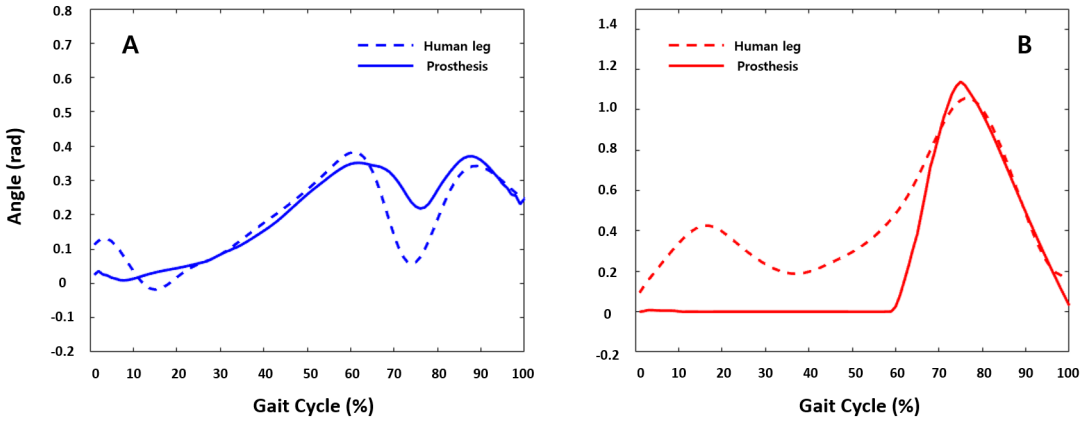

Figure 5.3: Comparison between the prosthesis' and the human walking on -10° inclination (A: Ankle joint, B: Knee joint)

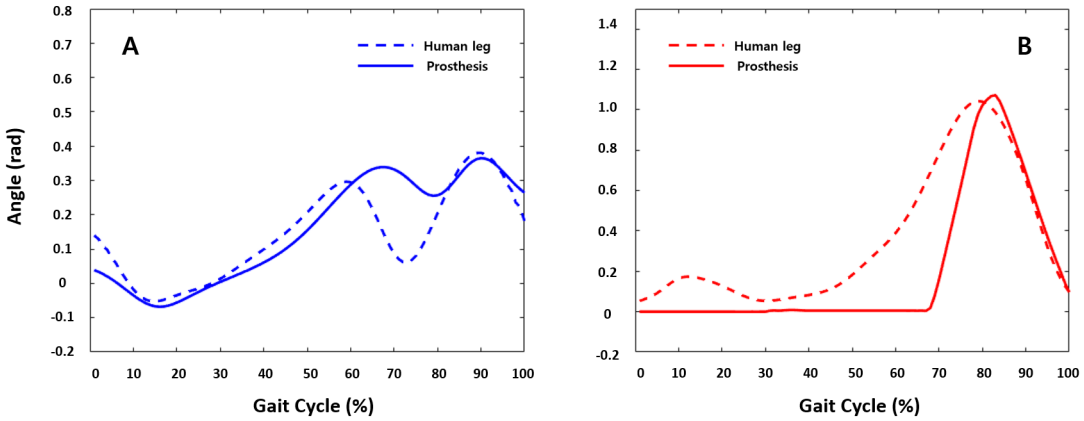

Figure 5.4: Comparison between the prosthesis' and the human walking on -5° inclination (A: Ankle joint, B: Knee joint)

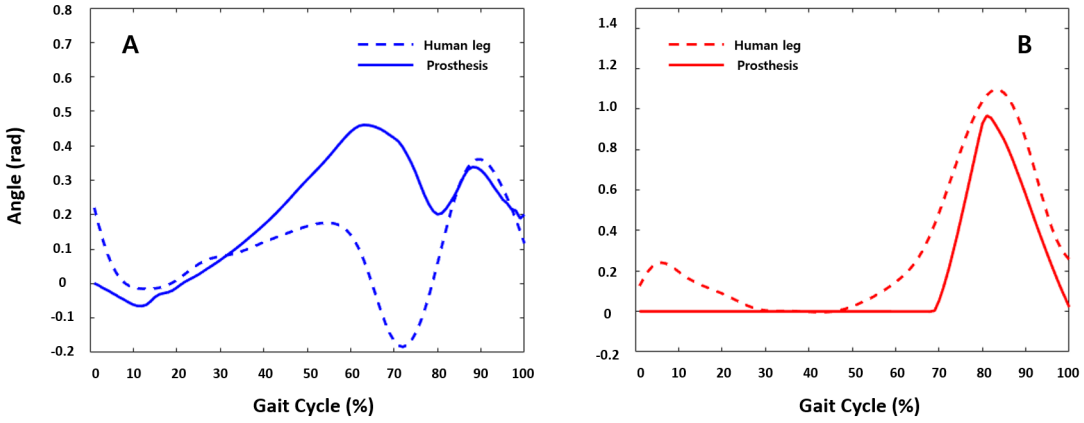

Figure 5.5: Comparison between the prosthesis' and the human walking on Flat-ground (A: Ankle joint, B: Knee joint)

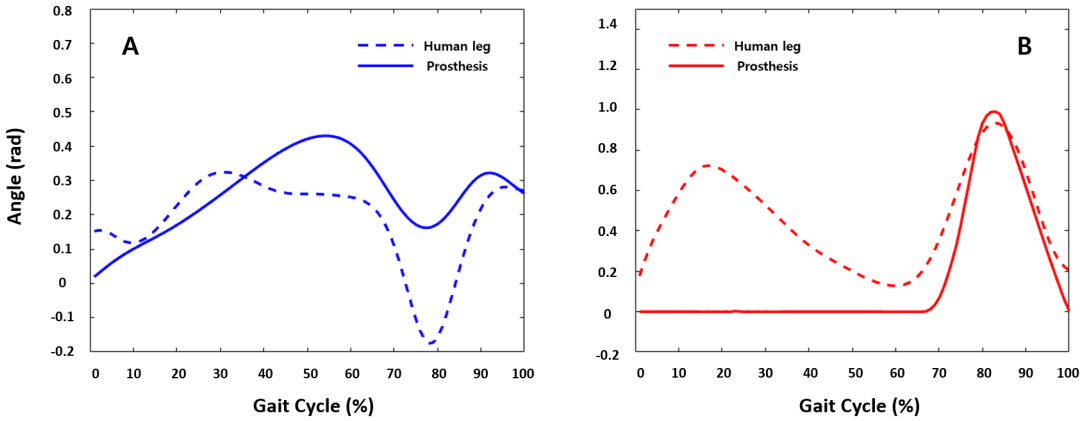

Figure 5.6: Comparison between the prosthesis' and the human walking on 5° inclination (A: Ankle joint, B: Knee joint)

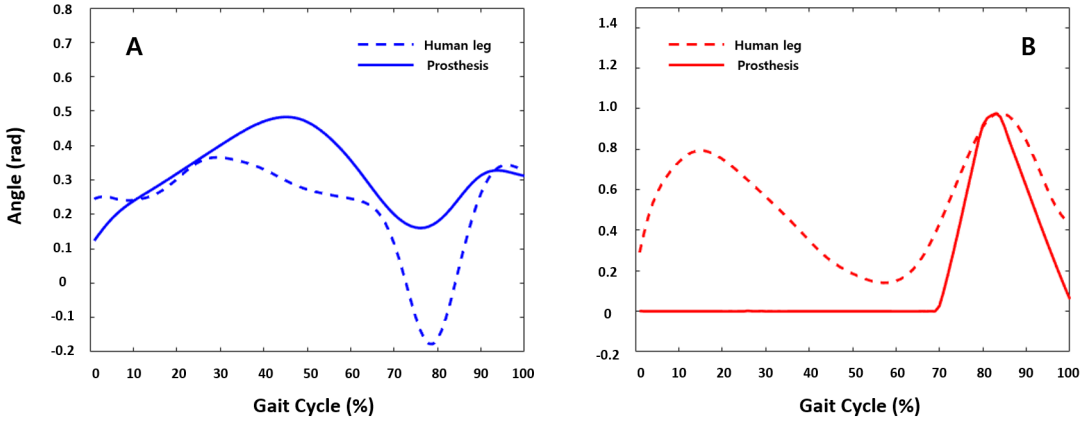

Figure 5.7: Comparison between the prosthesis' and the human walking on 10° inclination (A: Ankle joint, B: Knee joint)

Figure 5.8: Downslope walking on the treadmill (-10° inclination)

Figure 5.9: Downslope walking on the treadmill (-5° inclination)

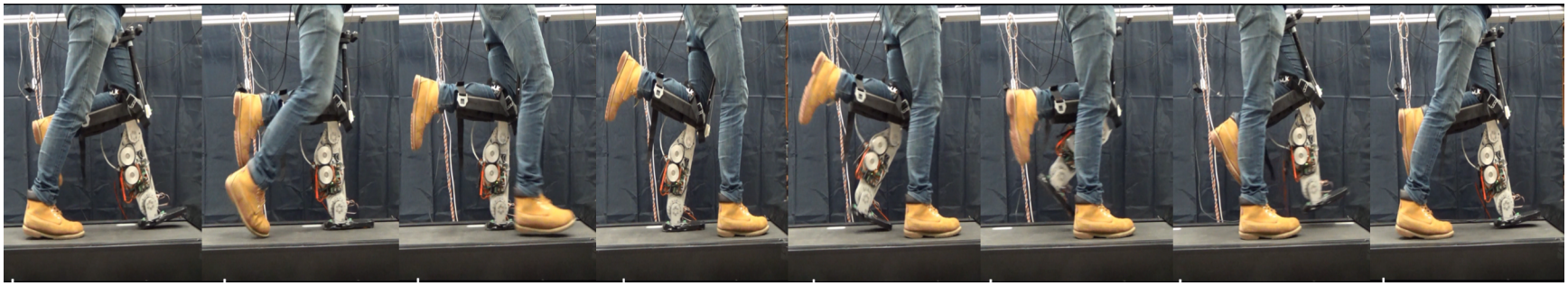

Figure 5.10: Flat-ground walking on the treadmill

Figure 5.11: Upslope walking on the treadmill (5° inclination)

Figure 5.12: Upslope walking on the treadmill (10° inclination)

6. FUTURE WORKS

To verify this framework in a different perspective, bio-mechanical analysis will be planned with the current prosthesis. By checking the energy expenditure and the metabolic cost of transport during test with the prosthesis, the control strategy will be further validated in a bio-mechanical perspective. Since the current device has no elastic components on the body, the user experience high impact at heel strike. To compensate for the impact at heel strike, elastic components will be included in the next generation of the transfemoral prosthesis. Also, there is no significant push-off since the current foot is a rigid flat-foot. This can be improved by dividing the foot into two parts: toe and foot, and putting some elastic components between them. Furthermore, in order to adapt to the ground more easily, one more degree of freedom, inversion and eversion, will be provided to the system. In the current framework, the device cannot accommodate different heights of the users because of its rigid frame. To overcome this limitation, an adjustable pylon can be utilized in the frame of the next prosthesis.

7. CONCLUSION & DISCUSSION

The proposed framework for the inclined walking allows the lower limb prosthesis to overcome the difficulties of inclined walking in real-time. Regardless of the slope information, appropriate joint trajectories can be generated from the suggested algorithm, and can be tracked using a PD controller with user comfort based gain value during the swing phase. An impedance controller is implemented for the stance phase. In this framework, cubic-Bezier-polynomials are chosen to provide enough freedom to generate different curved trajectories as the inclination varies. The required parameters for the Bezier-polynomials are solved by an off-line optimization problem – resulting in a simple polynomial equation that is solved by the prosthesis in real-time.

REFERENCES

[1] “Classification of lower limb amputation.” URL: "http://www.cdha.nshealth.ca /amputee-rehabilitation-musculoskeletal-program/patient-family-information/lower-limb-amputations", Accessed: 07/17/2017.

[2] “Waterproof passive prosthesis.” URL: "http://www.ottobockus.com/prosthetics/lower-limb-prosthetics/solution-overview/aqualine-waterproof-above-knee-system/", Accessed: 07/20/2017.

[3] “C-leg above knee prosthetic leg.” URL: "http://www.ottobockus.com/C-Leg.html", Accessed: 07/25/2017.

[4] B. E. Lawson and M. Goldfarb, “Impedance & admittance-based coordination congtrol for robotic lower limb,” *MECHANICAL ENGINEERING*, vol. 136, no. 9, pp. 62–67, 2014.

[5] H. Zhao, J. Reher, J. Horn, V. Paredes, and A. D. Ames, “Demonstration of locomotion with the powered prosthesis ampro utilizing online optimization-based control,” in *Proceedings of the 18th International Conference on Hybrid Systems: Computation and Control*, pp. 305–306, ACM, 2015.

[6] V. Paredes, W. Hong, S. Patrick, and P. Hur, “Upslope walking with transfemoral prosthesis using optimization based spline generation,” in *Intelligent Robots and Systems (IROS), 2016 IEEE/RSJ International Conference on*, pp. 3204–3211, IEEE, 2016.

[7] “Effects of amputation.” URL: "http://www.seriousinjurylaw.co.uk/other-serious-claims/amputation/effects-of-amputation", Accessed: 07/17/2017.

[8] D. G. Smith, “The transfemoral amputation level, part 1,” 2004. URL: "http://www.amputee-coalition.org /resources/transfemoral-amputation-part-1", Accessed: 07/17/2017.

[9] T. R. Dillingham, L. E. Pezzin, and E. J. MacKenzie, “Limb amputation and limb deficiency: epidemiology and recent trends in the united states,” *Southern medical journal*, vol. 95, no. 8, pp. 875–884, 2002.

[10] L. D. Patti Ephraim, “People with amputation speak out,”

[11] E. M. Ficanha, M. Rastgaar, and K. R. Kaufman, “A two-axis cable-driven ankle-foot mechanism,” *Robotics and Biomimetics*, vol. 1, no. 1, p. 17, 2014.

[12] E. J. Rouse, N. C. Villagaray-Carski, R. W. Emerson, and H. M. Herr, “Design and testing of a bionic dancing prosthesis,” *PloS one*, vol. 10, no. 8, p. e0135148, 2015.

[13] E. C. Honert and K. E. Zelik, “Whole-body walking biomechanics with vs. without a toe joint: implications for prosthetic foot design,”

[14] F. Sup, A. Bohara, and M. Goldfarb, “Design and control of a powered transfemoral prosthesis,” *The International journal of robotics research*, vol. 27, no. 2, pp. 263–273, 2008.

[15] F. Sup, H. A. Varol, and M. Goldfarb, “Upslope walking with a powered knee and ankle prosthesis: initial results with an amputee subject,” *IEEE Transactions on Neural Systems and Rehabilitation Engineering*, vol. 19, no. 1, pp. 71–78, 2011.

[16] B. E. Lawson, H. A. Varol, A. Huff, E. Erdemir, and M. Goldfarb, “Control of stair ascent and descent with a powered transfemoral prosthesis,” *IEEE Transactions on Neural Systems and Rehabilitation Engineering*, vol. 21, no. 3, pp. 466–473, 2013.

[17] R. W. Sinnet, M. J. Powell, R. P. Shah, and A. D. Ames, "A human-inspired hybrid control approach to bipedal robotic walking," *IFAC Proceedings Volumes*, vol. 44, no. 1, pp. 6904–6911, 2011.

[18] A. D. Ames, "First steps toward automatically generating bipedal robotic walking from human data," in *Robot Motion and Control 2011*, pp. 89–116, Springer, 2012.

[19] H. Zhao, J. Reher, J. Horn, V. Paredes, and A. D. Ames, "Realization of nonlinear real-time optimization based controllers on self-contained transfemoral prosthesis," in *Proceedings of the ACM/IEEE Sixth International Conference on Cyber-Physical Systems*, pp. 130–138, ACM, 2015.

[20] A. Hereid, C. M. Hubicki, E. A. Cousineau, J. W. Hurst, and A. D. Ames, "Hybrid zero dynamics based multiple shooting optimization with applications to robotic walking," in *Robotics and Automation (ICRA), 2015 IEEE International Conference on*, pp. 5734–5740, IEEE, 2015.

[21] A. S. McIntosh, K. T. Beatty, L. N. Dwan, and D. R. Vickers, "Gait dynamics on an inclined walkway," *Journal of biomechanics*, vol. 39, no. 13, pp. 2491–2502, 2006.

[22] W. Hong and P. Hur, "Transfemoral prosthesis control for slope walking with principal component analysis," in *American Society of Biomechanics (ASB) 2017*, pp. 841–842, American Society of Biomechanics (ASB), 2017.

[23] J. Shlens, "A tutorial on principal component analysis," *arXiv preprint arXiv:1404.1100*, 2014.

[24] A. D. Ames, "Human-inspired control of bipedal walking robots," *IEEE Transactions on Automatic Control*, vol. 59, no. 5, pp. 1115–1130, 2014.

[25] E. R. Westervelt, J. W. Grizzle, and D. E. Koditschek, "Hybrid zero dynamics of planar biped walkers," *IEEE transactions on automatic control*, vol. 48, no. 1, pp. 42–

56, 2003.

[26] E. R. Westervelt, J. W. Grizzle, C. Chevallereau, J. H. Choi, and B. Morris, *Feedback control of dynamic bipedal robot locomotion*, vol. 28. CRC press, 2007.

[27] M. A. Holgate, T. G. Sugar, and A. W. Bohler, "A novel control algorithm for wearable robotics using phase plane invariants," in *Robotics and Automation, 2009. ICRA'09. IEEE International Conference on*, pp. 3845–3850, IEEE, 2009.

[28] D. J. Villarreal and R. D. Gregg, "A survey of phase variable candidates of human locomotion," in *Engineering in Medicine and Biology Society (EMBC), 2014 36th Annual International Conference of the IEEE*, pp. 4017–4021, IEEE, 2014.

[29] D. J. Villarreal and R. D. Gregg, "Unified phase variables of relative degree two for human locomotion," in *Engineering in Medicine and Biology Society (EMBC), 2016 IEEE 38th Annual International Conference of the*, pp. 6262–6267, IEEE, 2016.

[30] N. Hogan, "Impedance control: An approach to manipulation," in *American Control Conference, 1984*, pp. 304–313, IEEE, 1984.

[31] N. Aghasadeghi, H. Zhao, L. J. Hargrove, A. D. Ames, E. J. Perreault, and T. Bretl, "Learning impedance controller parameters for lower-limb prostheses," in *Intelligent robots and systems (IROS), 2013 IEEE/RSJ international conference on*, pp. 4268–4274, IEEE, 2013.

[32] E. J. Rouse, L. J. Hargrove, E. J. Perreault, and T. A. Kuiken, "Estimation of human ankle impedance during walking using the perturberator robot," in *Biomedical Robotics and Biomechatronics (BioRob), 2012 4th IEEE RAS & EMBS International Conference on*, pp. 373–378, IEEE, 2012.

[33] H. Lee, E. J. Rouse, and H. I. Krebs, "Summary of human ankle mechanical impedance during walking," *IEEE journal of translational engineering in health and*

medicine, vol. 4, pp. 1–7, 2016.

[34] E. J. Rouse, L. J. Hargrove, M. A. Peshkin, and T. A. Kuiken, "Design and validation of a platform robot for determination of ankle impedance during ambulation," in *Engineering in Medicine and Biology Society, EMBC, 2011 Annual International Conference of the IEEE*, pp. 8179–8182, IEEE, 2011.

[35] N. P. Fey, A. M. Simon, A. J. Young, and L. J. Hargrove, "Controlling knee swing initiation and ankle plantarflexion with an active prosthesis on level and inclined surfaces at variable walking speeds," *IEEE journal of translational engineering in health and medicine*, vol. 2, pp. 1–12, 2014.